Molecularly imprinted polymer-based electrochemical sensors for environmental analysis

Patrícia Rebelo[a, c], Estefanía Costa-Rama[a,b]*, Isabel Seguro[a], João G. Pacheco[a], Henri P.A. Nouws[a], M. Natália D.S. Cordeiro[c], Cristina Delerue-Matos[a]

[a] REQUIMTE/LAQV, Instituto Superior de Engenharia do Porto, Instituto Politécnico do Porto, Dr. António Bernardino de Almeida 431, 4200-072 Porto, Portugal
[b] Departamento de Química Física y Analítica, Universidad de Oviedo, 33006 Oviedo, Spain
[c] REQUIMTE/LAQV, Departamento de Química e Bioquímica, Faculdade de Ciências, Universidade do Porto, Rua do Campo Alegre, s/n, 4619-007 Porto, Portugal

*e-mail: costaestefania@uniovi.es

Abstract

The ever-increasing presence of contaminants in environmental waters is an alarming issue, not only because of their harmful effects in the environment but also because of their risk to human health. Pharmaceuticals and pesticides, among other compounds of daily use, such as personal care products or plasticisers, are being released into water bodies. This release mainly occurs through wastewater since the treatments applied in many wastewater treatment plants are not able to completely remove these substances. Therefore, the analysis of these contaminants is essential but this is difficult due to the great variety of contaminating substances. Facing this analytical challenge, electrochemical sensing based on molecularly imprinted polymers (MIPs) has become an interesting field for environmental monitoring. Benefiting from their superior chemical and physical stability, low-cost production, high selectivity and rapid response, MIPs combined with miniaturized electrochemical transducers offer the possibility to detect target analytes in-situ. In most reports, the construction of these sensors include nanomaterials to improve their analytical characteristics, especially their sensitivity. Moreover, these sensors have been successfully applied in real water samples without the need of laborious pre-treatment steps. This review provides a general overview of electrochemical MIP-based sensors that have been reported for the detection of pharmaceuticals, pesticides, heavy metals and other contaminants in water samples in the past decade. Special attention is given to the construction of the sensors, including different functional monomers, sensing platforms and materials employed to achieve the best sensitivity. Additionally, several parameters, such as the limit of detection, the linear concentration range and the type of water samples that were analysed are compiled.

Keywords: molecularly imprinted polymer; electrochemical sensors; emerging contaminants; pharmaceuticals; pesticides; heavy metals.

1. Introduction

Pollution is defined as the direct or indirect introduction of substances or energy into the environment, by man, that are liable to cause harm to human health, living resources or the biosphere's ecological and physical systems (Holdgate, 1979; Khanmohammadi et al., 2020; Manisalidis et al., 2020). Although pollutants can also enter the environment through natural processes, such as volcanic activity, this definition, contained in EU legislation (Directive, 2008/1/EC), assigns environmental responsibilities to human activities. Besides the evident detrimental effects (such as loss of biological diversity, introduction of invasive species, excessive amounts of hazardous chemicals in the food chain, and global climate change), environmental

pollution is a major cause of illness that leads to great economic costs for health care systems. The terms pollution and contamination are sometimes used as synonyms but they are not really the same. A contaminant is a substance that is not normally present in the environment or that is present in concentrations above the natural background but is not necessarily harmful. On the other hand, a pollutant is a contaminant that results in harmful effects to the environment or living organisms (Chapman, 2007). However, in some cases this distinction is a bit fuzzy because harmful effects may occur but are not observed. Over the past decades, the rise in population, globalisation, and industrialisation have led to the dissemination and the increase of the amount and the variety of hazardous substances in the environment. The harmful effects to living organisms and the ecosystem of many of these substances, which range from heavy metals and pesticides to phenolic compounds, xenobiotics, plasticisers and antibiotics, have been demonstrated (Chakraborty et al., 2020; Dulio et al., 2018; Richardson and Ternes, 2014). However, there is still insufficient knowledge about the toxicity of some of them to environmental, animal and human populations.

Among these substances, the so-called "contaminants of emerging concern" (CECs) or "emerging contaminants" are receiving huge attention because of their increasing presence and extensive distribution in the environment (Dulio et al., 2018; Kroon et al., 2020; Naidu et al., 2016; Petrie et al., 2014). CECs, and their metabolites and/or transformation products, are a heterogeneous group of compounds that are present in a wide variety of products, including industrial chemicals, pharmaceuticals, drugs of abuse, personal care products, biocides, food additives, surfactants and plasticisers (Dulio et al., 2018; Lapworth et al., 2012; Ramírez-Malule et al., 2020). The term CECs does not only cover newly developed substances but also chemicals that have entered the environment for years, whose presence has only recently been detected (either because of the increase of their concentration or because of the advances in analytical methods) and/or studied (Richardson and Ternes, 2014; Zulkifli et al., 2018). Due to insufficient knowledge about the toxicity, impact, and behaviour of CECs, many of them are not yet regulated, so they are not routinely monitored and submitted to an emission control regulation. However, since their potential negative effects are increasingly recognised, relevant regulations are expected over the next years (Bilal et al., 2019). The variety and amount of CECs is so impressive that the list of priority substances created by NORMAN (the network of reference laboratories, research centres and related organisations for monitoring of emerging environmental substances funded by the European Commission) includes more than 900 (Dulio et al., 2018; norman-network).

Although CECs can enter the environment by the same routes as traditional contaminants, such as industrial processes and emissions, wastewater is recognised as a highly important contributor to the entry of CECs in the aquatic environment (Lapworth et al., 2012; Luo et al., 2014; Paíga et al., 2016), especially in countries/regions which do not have suitable regulation regarding wastewater treatment. However, even in regions with adequate regulation, removal of CECs may be incomplete because this largely depends on the physical-chemical characteristics of the contaminants and on the treatments applied in the wastewater treatment plants (WWTPs) (Lapworth et al., 2012; Luo et al., 2014; Patel et al., 2019). Other important sources of the release of CECs into the aquatic environment are landfill sites, since CECs may leach and reach groundwater, sewage sludge, and manure (that may contain veterinary pharmaceuticals) used in agriculture (Lapworth et al., 2012; Sui et al., 2015). Therefore, the determination of CECs levels in the aquatic environment is of great importance, not only to evaluate the water quality and security, but also to improve the knowledge on their pathways and fate.

As mentioned previously, the increasing amount and variety of contaminants has led to more stringent environmental regulations and, consequently, to the increase of the demands on environmental analysis. Vice versa, the latest improvements in environmental analysis results in legislation stringency. The analysis of contaminants in waters involves great challenges since they are a very large group with very different physical/chemical properties that are present at very low concentrations (Geissen et al., 2015; Rasheed et al., 2019). In this context, powerful analytical techniques (e.g. high-performance liquid chromatography and gas chromatography coupled to mass spectrometric detection (HPLC-MS and GC-MS, respectively) (Arismendi et al., 2019; Beldean-Galea et al., 2020; Benedetti et al., 2020; Liang et al., 2020; Merlo et al., 2020; Paíga et al., 2019) are used for the detection of contaminants in waters. However, these techniques are often not as fast and cost-effective as desired since they require complex and expensive instrumentation, laborious sample pre-treatment procedures and long analysis times (Rasheed et al., 2019; Zulkifli et al., 2018).

Spatial and temporal variations are also important issues in environmental analysis due to seasonality, inter- and intra-day variations and occasional events that can hamper a harmonised and representative screening (Luo et al., 2014; Paíga et al., 2019). Therefore, complete information of the presence of contaminants in water bodies and its spatial and temporal distribution requires the collection of several samples at different times. When conventional analytical methodologies, such as solid phase extraction followed by chromatographic analysis (Kuhn et al., 2020), are used, these samples must be sent to a laboratory, turning real-time information impossible. Hence, there is the need to develop technological solutions for easy, fast and on-site contamination monitoring that provide a representative spatial-temporal picture of environmental quality.

The growing demand for inexpensive and easy-to-use analytical devices capable of rapidly providing valuable qualitative and quantitative on-site information increases the interest in electrochemical sensors because of their reduced size, portability, low cost and low reagent and sample consumption. Moreover, the combination of cutting-edge technologies in digital communication networks and innovative sensors allows the construction of smart analytical tools. A robust electrochemical sensor requires the successful integration of a transducer (usually an electrochemical cell comprising a working- a reference- and a counter electrode) with a recognition element (e.g. biological (enzyme, antibody, protein…) or artificial (e.g. molecularly imprinted polymers (MIPs)). MIPs have attracted wide attention as recognition elements for sensor development due to their high selectivity towards the target analyte and their advantages compared to biological receptors: i) easy and low-cost preparation, ii) physical and chemical robustness when unfavourable conditions are used, such as organic solvents, extreme pH values, high temperatures and/or high pressures, iii) reusability, iv) stability and v) possibility of large scale production (Ansari and Karimi, 2017a; Figueiredo et al., 2016; Gui et al., 2018).

The basis of today's molecular imprinting technology (MIT) started with the studies presented by Wulff and Sarhan (1972) almost 50 years ago (Beluomini et al., 2019). In the first decades the development and application of MIPs were mainly focused on separation and extraction techniques. Nowadays, MIPs are used in a wide variety of applications (Belbruno, 2019; Chen et al., 2016) including sample preparation (e.g. solid phase extraction) (Ansari and Karimi, 2017b), chromatographic separation (Boysen, 2019; Yang et al., 2016), drug delivery (Han et al., 2019; Luli´nski, 2017; Mokhtari and Ghaedi, 2019) and chemical sensing (Cai et al., 2019; Lopes et al., 2017; Pacheco et al., 2018; Rebelo et al., 2020). Electropolymerisation has facilitated the application of MIPs in electrochemical sensing by employing electroactive monomers that can polymerize by applying electric current. The first studies of selective MIPs towards several species produced in this way were done by Boyle et al. (1989), Dong et al. (1988) and Vinokurov (1992). After this, the first combination of electropolymerised MIPs and sensors was described by Hutchins and Bachas (1995) for the analysis of nitrate using a potentiometric sensor. The electrochemical synthesis approach was also successfully used to develop MIP-sensors by two different groups in 1999 (Deore et al., 1999; Malitesta et al., 1999). Malitesta et al. (1999) proposed the electropolymerisation of o-phenylenediamine (o-PD) in the presence of glucose (neutral molecule) in an aqueous environment on a gold-coated quartz crystal to assemble a piezoelectric sensor. Deore et al. (1999) reported the electrochemical preparation of polypyrrole (PPy) imprinted with L-glutamate anion. Along with electropolymerisation, the modification of electrodes with MIPs prepared by traditional methods such as bulk polymerisation was also explored. More recently, the MIP technology has been coupled to disposable and miniaturized screen-printed electrodes. So, in the future it is foreseen that some MIPs could be used in commercial sensing solutions.

Theoretically, MIPs can be prepared for any molecule of interest; indeed, the MIP database (available at http://mipdatabase.com) compiles MIPs for more than 10,000 target molecules. Therefore, in the last decade, the development of MIP-based electrochemical sensors has exploded as well as the concern about emerging contaminants (Fig. 1) (Ahmad et al., 2019; Ansari and Karimi, 2017a; Beluomini et al., 2019; Gui et al., 2018; Lahcen and Amine, 2019). Combining MIPs and electrochemical sensing strategies has shown great potential to benefit environmental pollution control (Ayankojo et al., 2020).

In this work, a comprehensive review of MIP-based electrochemical sensors for the analysis of contaminants in water is provided. There are some recent reviews about this kind of sensors, however, they are general regarding the applications of the sensors (Beluomini et al., 2019; Gui et al., 2018; Lahcen and Amine, 2019), or they are focused on the preparation and use of imprinted polymers for recognition and extraction, not only in sensing applications but also in solid phase (micro) extraction (Ansari and Karimi, 2017a; Figueiredo

et al., 2016). Thus, this review includes a summary of the main environmental contaminants and provides a general overview of the MIP-based electrochemical sensors reported for the analysis of these contaminants in water samples focusing on the polymerisation technique, functional monomers, types of electrodes and electrode modifiers and comparing their performances. Finally, the present challenges and prospects for advancing the use of this kind of sensors for environmental analysis are discussed.

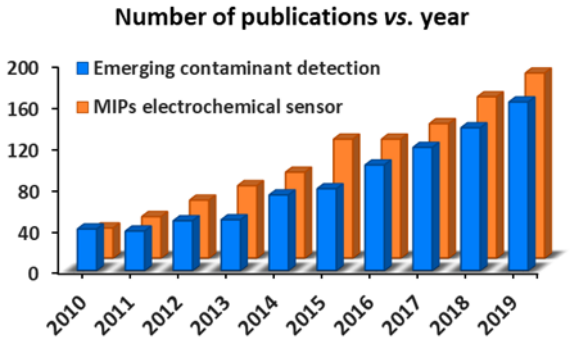

Figure 1. Evolution of publications regarding MIP-based electrochemical sensors and emerging contaminant detection in the last 10 years.

2. MIPs as recognition elements for electrochemical sensors

MIPs are tailor-made synthetic materials with selective binding cavities that act as recognition sites for a specific target molecule, mimicking natural receptors (Chen et al., 2016). MIPs are synthesized by mixing the template molecule with a functional monomer in an inert porogenic solvent, resulting in the formation of a pre-polymerisation complex. This complex polymerises in the presence of a cross-linking agent (that fixes the monomer around the template and allows the generation of the three-dimensional polymer network) and an initiator. After completion of the polymerisation process, the template is removed from the polymeric matrix leaving specific cavities whose shape, size and functional groups are complementary to the template molecule. Therefore, a molecular memory is generated inside the polymer, in which the target molecule is now able to rebind with a very high specificity. In this way, the MIP acquires the ability to selectively recognise the target molecule in the presence of other closely related molecules; a process that is very similar to the "lock and key" mechanism of enzymes (Chen et al., 2016; Madikizela et al., 2018a). A schematic summary of preparation of a MIP, signal enhancement strategies and detection mechanisms in electrochemical sensors is shown in Fig. 2.

The recognition properties of a MIP are compared with a non-imprinted polymer (NIP) that is prepared in the same conditions, but without the inclusion of the template molecule. Obviously, the great challenge is to obtain a MIP with the highest selectivity for the target molecule (Arrigo and Baroni, 2020).

The necessity of quantifying very low contaminant concentrations, the complexity of environmental samples and the limited availability of sensitive and selective methods are the principal difficulties for environmental monitoring (Madikizela et al., 2018b; Madikizela et al., 2018c; Namiesnik, 2000; Spietelun et al., 2013). In this context, suitable sample preparation techniques have been applied to selectively isolate and preconcentrate the analytes prior to their determination (Sarafraz-Yazdi et al., 2012). Many research papers have shown the use of MIPs as selective sorbents for extraction of various contaminants from complex sample matrices (Madikizela et al., 2018c). Despite the advantages of this advanced technical application of MIPs, they are also excellent tools to be used as recognition elements in electrochemical sensing (Li et al., 2019b). As mentioned before, when compared with biological receptors, such as antibodies or enzymes, MIPs are cheaper, more robust and have a greater reusability. However, the optimisation of the synthesis process to obtain a selective MIP is often a laborious and time-consuming task that not always leads to a suitable MIP as recognition element in a sensor. In this context, to avoid the extent and trial-and-error of experimental procedures, computational simulations have been employed to describe, predict and analyse molecular

imprinting systems (Zhang et al., 2019). With a sustainable strategy, strong guidance regarding on the design of MIPs (Khan et al., 2019; Rebelo et al., 2020; Xie et al., 2020).

Because of the differences in the templates' properties and the potential applications of the MIPs, a great variety of strategies for their preparation, such as bulk, suspension, emulsion and precipitation polymerisation, and surface imprinting, have extensively been reviewed (Ansari and Karimi, 2017b; Belbruno, 2019; Chen et al., 2016; Ertürk and Mattiasson, 2017; Lahcen and Amine, 2019; Mayes and Whitcombe, 2005). In the case of MIP-based electrochemical sensors, there are different approaches for the integration of the MIPs with the transducer (Gui et al, 2018, 2019; Toro et al., 2015). The main ones are i) the mixture of the MIP with the material of the working electrode before the preparation of the electrode; ii) the immobilisation (usually by drop coating) of a previously prepared MIP or MIP-based composite with conductive/nanomaterials on the transducer surface; and iii) electropolymerisation. These synthesis and integration strategies are reviewed in the next sub-section.

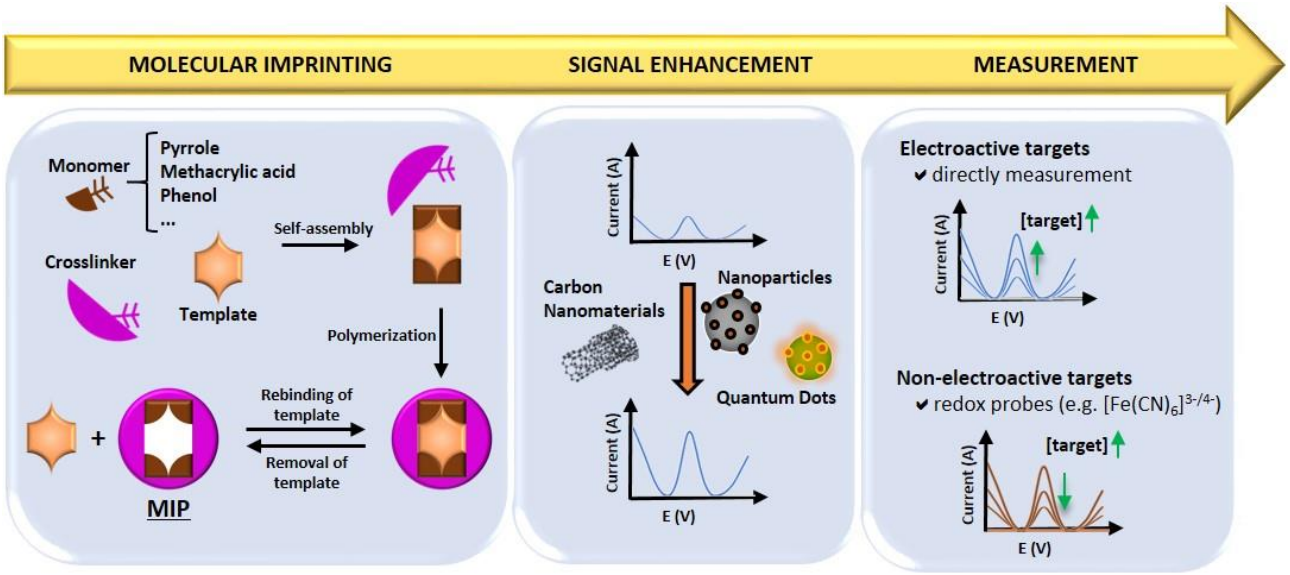

Figure 2. Summary of the preparation procedure, signal enhancement and sensing mechanism of electrochemical MIP-based sensors.

2.1. Preparation processes of MIPs

In the classical MIP preparation methods mentioned above, the bond between the template and the monomer can either be covalent or non-covalent. Non-covalent binding is more flexible since the removal and subsequent rebinding of the template is easier (Zaidi, 2017; Zhou et al., 2019). Some problems that still need to be overcome are related to the elution of polar compounds, which have a low solubility in organic solvents, the reduced number of effective recognition sites, the slow mass transfer rate and the incompatibility of MIPs with aqueous media (Chen et al., 2011). So, alternative imprinting routes or new imprinting techniques are constantly being developed.

As mentioned in the introduction, theoretically, MIPs can be synthetized for any analyte, but there is no specific strategy for a particular class of analytes; i.e. the optimisation of the imprinting process by experimental studies is crucial to produce the best MIP (or the MIP with the desired characteristics) for the target molecule. Bulk polymerisation is the conventional and most popular approach due to its simple operation and low production costs. In this method, also known as mass polymerisation, the template, functional monomer, cross-linker and initiator are mixed in a single reactor (Farooq et al., 2018). This process results in a rigid monolithic polymer matrix that, after crushing and grinding, may have some shortcomings such as the loss of binding sites that can lead to a low yield (Chen et al., 2011; Farooq et al., 2018). Although there are different protocols for the preparation of MIPs by bulk polymerisation, this method follows a typical sequence involving five main steps: pre-polymerisation of the functional monomers with the template molecules, addition of the cross-linking agents and initiators, polymerisation by heating for an extend period of time, extraction of the template and crushing the crosslinked mass into power. Precipitation polymerisation, suspension polymerisation and emulsion polymerisation are three spherical MIP synthesis

methods. In these methods, the polymerisation procedure is similar to bulk polymerisation, but the post-treatment steps are not required, which reduces the number of steps and, more importantly, the probability of destroying the imprinted cavities (Chen et al., 2011; Xiao et al., 2018). Precipitation polymerisation is carried out in a large volume of an organic solvent in which the polymers are insoluble and precipitate. This method is free of surfactants and allows to control the size of the particles, but their shape remains irregular. Suspension and emulsion polymerisation are used to prepare micro spherical MIPs and to increase monodispersity. For emulsion polymerisation an oil/water biphasic system is prepared and surfactants are added to the organic phase to prevent diffusion across the continuous aqueous phase (Wackerlig and Schirhagl, 2016). Compared to the precipitation strategy, suspension and emulsion polymerisation require more reagents and the purity and performance of the products are affected by the presence of surfactants remnants (Chen et al., 2016).

Another process for the preparation of MIPs is surface imprinting, in which electropolymerisation is frequently used. In *in-situ* electropolymerisation, using cyclic voltammetry (CV), the imprinted polymers are produced by coating surfaces at a well-controlled rate, producing an ultrathin polymeric film. In this process, the CV cycles and time can be used to determine and regulate the adhesion and the morphology of the polymeric film on the surface of substrates, facilitating the optimisation of the synthesis and providing highly reproducible MIPs in terms of binding capacities and immobilisation on the substrate's surface. Moreover, this technique facilitates template removal since the obtained MIP film is thin and all the imprinting cavities are situated on or closely at the surface (Cieplak and Kutner, 2016). So, electropolymerisation is usually a simple and fast procedure involving three steps: solubilization and interaction of a functional monomer with the desired template in a solvent, and electrochemical coating followed by extraction of the template (Crapnell et al., 2019). Other strategies for surface imprinting have also been studied. For example, the sol-gel process is an approach that can facilitate MIP preparation in aqueous matrices (Moein et al., 2019; Zhou et al., 2019). This technique consists of the use of silica-based materials as supports that allow the use of green solvents and an easy construction at room temperature without the problem of chemical or thermal decomposition observed in bulk polymerisation (Moein et al., 2019; Pohanka, 2017; Zhou et al., 2019). There are two main steps for sol-gel processing: sequential hydrolysis of silane in the presence of an acidic or basic catalyst and condensation of a series of silane monomers to form siloxane bonds. With time, a porous and a strong three-dimensional network is formed by colloidal particles aggregation (Mujahid et al., 2010; Yang et al., 2013). Sol-gel materials offer high thermal stability and porosity, which combined with molecular imprinting systems play a significant role in the performance of MIPs. The lack of functional monomers, the low sensitivity, slow diffusion kinetics and long response times are some drawbacks of this process (Adumitrachioaie et al., 2018; Zhou et al., 2019).

Many materials for surface modification are also used in surface molecular imprinting processes such as Fe3O4 magnetic nanoparticles (Fe_3O_4 MNPs) and mesoporous SiO_2 nanoparticles (SiO_2 NPs) (Fig. 2). Besides a larger specific surface area, magnetic nanoparticles have superior advantages in the removal of solvents and in the fast and easy isolation of the analyte from samples by applying a magnetic field (Huang et al., 2018; Ye, 2013). SiO_2 NPs provide a stable solid support due to their mesoporous properties, allowing higher stability and sorption capacities in comparison with ordinary imprinting methods (Wang et al., 2011). By virtue of the controllable methods and ease of modification, surface imprinting technologies have been explored by several research groups. Furthermore, they have also included functional nanomaterials in the imprinted shell layers to improve the MIP-based sensors' electron transfer rates (Beluomini et al., 2019; Maduraiveeran et al., 2018). Carbon nanotubes (CNTs), graphene and quantum dots (QDs) have received special attention in the preparation of MIPs. Among the carbon materials, graphene is the most widely used because of its unique physicochemical properties. Besides its low electronic noise and thin 2-dimensional surface, graphene has strong interaction with carbon-based ring compounds, such as some contaminants (Zaidi, 2017). QDs are a kind of conducting nanocrystals that have excellent photoluminescence properties (Shi et al., 2019). QDs possess high luminescence efficiency and photostability, a broad absorption spectrum, narrow fluorescence emission bands and quantum-size effects (Nsibande and Forbes, 2019). The combination of their excellent properties with the specific recognition of MIPs is gaining more attention as an alternative for sensitive and selective detection of contaminants (Nsibande and Forbes, 2019; Sobiech et al., 2019; Wang et al., 2019; Zhou et al., 2018). Prior to molecular imprinting, QDs can be loaded on an

electrode surface or incorporated in the surface of supporting nanomaterials such as SiO2 NPs (Tan et al., 2016; Yola and Atar, 2017).

2.2 Functional monomers

The selection of an appropriate functional monomer is an essential step for the successful construction of MIPs with desired affinity and selectivity. Template-monomer interactions can be changed by the combination of different functional groups. So, many types of commercially available functional monomers have been studied, based on their potential to establish hydrogen bonds or electrostatic interactions with the template. Among the functional monomers reported in the literature, methacrylic acid (MAA), pyrrole (Py), and phenol (Ph) and derivates are the most widely used in electrochemical MIP-based sensors for the detection of contaminants. Due its nature, MAA is the most popular carboxylic acid-based monomer used in bulk polymerisation. MAA not has only the ability to serve as both hydrogen bond donor or acceptor, but it can also interact with the template in various ways, including strong ion-pair and dipole-dipole interactions, and van der Waals forces, increasing its broad applicability (Mayes and Whitcombe, 2005). Py is a conductive (to some extent) and electropolymerisable monomer, well known to partially cross-link (Sadriu et al., 2020). Without the need to add a cross-linker, electropolymerisation is the most efficient method to synthesize PPy MIPs. The formation of the PPy film is fast, and a chemically and mechanically stable polymer is obtained (Sadriu et al., 2020). As a result of its good permeability, the use of PPy also allows easier extraction and rebinding of the template. Nevertheless, there are several experimental variables that can affect the chemical and physical properties of PPy formed on the electrode's surface, such as solvent, electrolyte, temperature and pH (Sadki et al., 2000). In contrast, Ph and p-aminothiophenol (PATP) are electronically non-conducting polymers which are also extensively used in electropolymerisation. The insulation properties of the formed polymer films can be improved by using self-assembled monolayers (Sharma et al., 2012); particularly PATP, which contains thiol groups, has been used for strong binding on gold surfaces. All these functional monomers can establish strong hydrogen bonds with templates, demonstrating that this effective interaction is a promising option to take into account during MIP preparations (Ansari, 2017).

2.3 Detection mechanisms

When using electrochemical MIP-based sensors, electrical signal (current or potential) changes, which are proportional to the concentration of the target analyte, are recorded (Li et al., 2012). Two principal techniques are used to detect the specific recognition events: voltammetry and electrochemical impedance spectroscopy (EIS) (Li et al, 2019b).

The voltammetric methods include linear sweep voltammetry (LSV), CV, differential pulse voltammetry (DPV) and square wave voltammetry (SWV). In these methods, the electroactivity of the analyte conditions the detection mechanism. For electroactive molecules, the current is measured directly, where the signal outputs ideally are the faradaic currents resulting from the oxidation/reduction of the analytes after binding in the MIP. In this case, under controlled conditions a correlation can be made between the concentration of the analyte and the measured current (Chen et al., 2016). When non-electroactive targets are involved, the signal can be produced using redox probes such as $[Fe(CN)_6]^{3-/4-}$ (Li et al., 2012). In this case, also called the "gate-controlled" mechanism, the current response of the redox probe is inversely proportional to the concentration of the analyte since higher concentrations lead to fewer channels for the diffusion of the redox probe to the electrode surface, and consequently to the decrease of the signal (Gui et al., 2019) (Fig. 2).

EIS is a powerful tool to investigate electron transfer and diffusion processes that occur at the electrode/electrolyte interface. The typical Nyquist plot obtained in EIS has two areas: at high frequencies a semi-circle portion corresponds to the electron transfer resistance, and at low frequencies diffusion limited process are observed by a linear portion (Li et al., 2018). During the MIP's assembly process, changes in the surface properties of the electrode occur and different Nyquist plots are observed. Generally, the rebinding of the template in the cavities of the polymeric film results in an increase of the charge transfer resistance on the surface of the electrode, thus semi-circles with larger diameters are observed.

3. MIP-based electrochemical sensors for contaminant analysis

3.1 Pharmaceuticals

Pharmaceuticals are widespread micropollutants and are ubiquitous in waters and soils (Afonso-Olivares et al., 2017; Kamba et al., 2017). They have been released into the environment for decades through various ways, such as metabolic excretion in its original form or as metabolites, improper disposal of expired medication, and escaping the modest removal efficiencies of WWTPs (Bj¨orlenius et al., 2018; Rivera-Jaimes et al., 2018). Despite their low concentrations, their long half-lives amplifies effects from drug-drug interactions that can potentially be hazardous (Evgenidou et al., 2015; Kamba et al., 2017). Subtle effects of pharmaceutical compounds on aquatic and terrestrial organisms have been reported (Boxall, 2004) and, more recently, a major concern of the public and the scientific community includes bacterial resistance (Ayukekbong et al., 2017; Richardson and Ternes, 2014).

There is no definitive date that marks the emergence of the identification of pharmaceuticals in the environment (Daughton, 2016), but over the past three decades various methods and approaches have been developed to assess their profiles and occurrence patterns in different environmental compartments (Evgenidou et al., 2015; Yang et al., 2017). Undoubtedly, the knowledge of concentration levels of pharmaceuticals is essential as a starting point to apply more advanced treatments to improve their removal and, consequently, minimise their environmental risk (Afonso-Olivares et al., 2017).

Since 2009 several works have been dedicated to the development of electrochemical MIP-based sensors for the determination of a wide variety of pharmaceuticals including antibiotics, anti-inflammatories, analgesics, hormones, blood lipid regulators, β-blockers, antidepressants, antiepileptics and cytostatic drugs (Des Azevedo et al., 2013; Florea et al., 2015; Futra et al., 2016; Han et al., 2016; Miege et al., 2009; ¨Ozcan and Topçuo˘gulları, 2017; Xiao et al., 2017; Yang et al., 2017). Many different strategies based on new imprinting techniques and polymerisation methods, and the use of innovate nanomaterials have been studied to improve the performance of the sensors (Adumitrachioaie et al., 2018; Uzun and Turner, 2016). However, only a few electrochemical MIP-based sensors were applied to environmental samples. This is mainly because of the low levels of contaminants in the environment. Table 1 summarises the main characteristics of electrochemical MIP-based sensors for the detection of different classes of pharmaceuticals in water samples.

3.1.1 Antibiotics

Antibiotics are the most frequently studied group of pharmaceuticals for electrochemical detection using MIP-based sensors, showing the concern about their presence in waters and the importance of their detection.

Sulfamethoxazole (SMX) is one of the most frequently sulfonamide bacteriostatic antibiotic detected in the aquatic environment, soils and sediments due to its wide spectrum of applications and poor ability to be metabolised (Fekadu et al., 2019; Tao et al., 2019; Zhao et al., 2015). SMX has been detected in industrial effluents, in WWTP effluents and in surface water at concentrations between 0.036 nM and 7.2 nM with detection frequencies of more than 80% (García-Espinoza and Mijaylova Nacheva, 2019). In Africa, it was the most detected compound in water samples, reaching concentrations far higher than the ecotoxicity endpoints (Fekadu et al., 2019). Its presence revealed high risk to sensitive aquatic organisms (Zhang et al., 2012) with possible mutagenic activity and the potential to disrupt the endocrine system (Archer et al., 2017; Zhao et al., 2015). Therefore, its monitoring is relevant to guarantee the health of all organisms. In 2015, the first electrochemical MIP-sensor, based on a PPy modified Boron Doped Diamond Electrode (BDDE), was developed for the determination of SMX in spiked lake water (Zhao et al., 2015). This sensor was prepared by electropolymerisation of Py and the determination of SMX was achieved through its direct oxidation using SWV. A good sensitivity, a limit of detection (LOD) of 24 nM and minimal interferences of structurally similar sulfonamides (sulfadimethoxine, sulfadiazine and sulfafurazole) were observed. Although BDDEs have excellent properties, some researchers avoid their use because of the very heterogeneous composition of the BDDE's surface (Feier et al., 2019) and because of the possibility of its degradation in alkaline solutions (Luong et al., 2009). Sulfanilamide (SN) is another member of the sulfonamide family and has mainly been

detected in surface waters, with high detection rates in Chinese rivers in comparison with other countries. Tadi et al. (2014) also used electropolymerisation of Py for the fabrication of a sensor for the analysis of SN. In this case, a pencil graphite electrode (PGE) was used. Py was selected as the best functional monomer compared with furan, thiophene, methyltiophene and methylpyrrole since computational studies showed it has the highest binding interaction energy with SN. DPV was used for its direct analysis (oxidation), achieving an LOD of 20 nM. This sensor showed good selectivity towards SN; species with analogue structures such as SMX, sulfathiazole and sulfadiazine did not significantly interfere in the analysis. The applicability of this sensor was tested in spiked human serum and ground water samples, obtaining recoveries between 98 and 115%.

The use of nanomaterials is one of the most widely used strategies to increase the electrode's surface area and consequently the sensitivity of the method. Zamora-Gálvez et al. (2016) reported a specific and highly sensitive composite-based sensing system, based on MIP-modified Fe3O4 MNPs, to detect SMX via EIS (Fig. 3A). In this work, nano-sized MIP cavities were constructed on the surface of the Fe3O4 nanoparticles by bulk polymerisation using MAA as the functional monomer. Because of the superparamagnetic properties of the formed composite, this sensing system allowed easy separation, pre-concentration and manipulation of the target analyte. After magnetic deposition of the composite on the surface of a screen printed carbon electrode (SPCE), the electron transfer resistance (Rct) was monitored by EIS in the presence of [Fe(CN)6]3-/4-, which increased with increasing SMX concentrations. This sensing system showed an excellent LOD of 1 × 10^{-3} nM and was applied to spiked seawater samples, achieving recoveries between 87 and 106%. In comparison with the previously described SMX sensor (Zhao et al., 2015), and although higher amounts of reagents were required, a much lower LOD was obtained. In this work MIP-modified Fe3O4 MNPs were used to separate and pre-concentrate SMX and their magnetic deposition onto the surface of SPCEs offered an innovative design in the field of disposable sensors.

Azithromycin (AZY) and erythromycin (ERY) are frequently prescribed macrolide antibiotics to treat many different bacterial infections. Due to their wide use, the difficulty of removing them by common wastewater treatments and their frequent detection in water bodies, AZY and ERY were included in the EU Watch List (Decision, 2018/840/ EU) of substances that could pose a significant risk to aquatic environments (Ayankojo et al., 2020; Rebelo et al., 2020). Recently, a low-cost and user-friendly electrochemical MIP sensor to detect AZY in water was reported (Rebelo et al., 2020). By a computational study based on density functional theory (DFT), 4-aminobenzoic acid (4-ABA) was chosen as the most suitable monomer, which was electropolymerised on the surface of a SPCE. The analysis of AZY was performed by its oxidation using DPV (LOD = 80 nM) and the sensor displayed great recognition behaviour in the presence of other interfering compounds. It was successfully applied to the analysis of spiked tap water and water samples collected upstream of a WWTP output in the Ave river (Portugal). A similar system was used by Ayankojo et al. (2020) to obtain the first ERY-selective MIP film integrated with a screen printed gold electrode (SPAuE). In their work, the MIP was generated directly on the SPAuE via electropolymerisation of m-phenylenediamine (m-PD). DPV measurements performed using a $[Fe(CN)_6]^{3-/4-}$ redox probe, allowed the determination ERY with an LOD of 0.1 nM.

Chloramphenicol (CAP), one of the oldest antibiotics, is widely used in veterinary medicine and to promote the growth of food-producing animals. This antibiotic was completely banned for use in food-producing animals in many European countries due to its potential serious adverse effects (Zhao et al., 2012). Despite legal bans, CAP is easily available and is still used because of economic interests (Ding et al., 2017; Shaheen et al., 2017). Zhao et al. (2012) reported the first electrochemical sensor for the determination of CAP in natural water samples, combining MIPs and the advantages of carbon nanotubes (CNTs) and gold nanoparticles (AuNPs). The functional monomer, diethylaminoethyl methacrylate (DMA), was added together with CAP to perform bulk polymerisation and the direct detection process was based on DPV using a glassy carbon electrode (GCE). The LOD of this sensor was 74 nM and the selectivity for CAP detection was demonstrated in the presence of penicillin-G, thiamphenicol and their analogue p-nitrophenol. Bulk polymerisation was also used to construct a novel sensor modified with chitosan and AuNPs (Ch-AuNPs) to detect ciprofloxacin (CIP), an antibiotic that has been detected in surface waters. Ch-AuNPS were used as the supporting material to polymerize MAA in the presence of CIP (Surya et al., 2020). The resulting MIP was drop casted onto the surface of a GCE and its capability to quantify the antibiotic in real samples was tested using mineral and tap water. Another antibiotic of the quinolone family that has also been detected in surface

waters is lomefloxacin (LFX).Li et al. (2020a) developed an effective MIP sensor for its determination in river waters. They used a gold electrode modified with Fe-doped porous carbon (Fe-PC) and electropolymerisation to produce the MIP film. Because of the hydrogen bonds and host-guest inclusion interactions, o-phenylenediamine (o-PD) and β-cyclodextrin (β-CD) were chosen as functional monomers. This methodology allowed high selectivity towards LFX, because of the use of the MIP prepared with bifunctional monomers, and high sensitivity, which was attributed to the large specific surface area, rich porosity, and good catalytic property of Fe-PC. An indirect detection approach and DPV were used for the analysis of LFX detection in river waters, achieving an LOD of 0.2 nM.

Table 1. Electrochemical MIP sensors constructed on different sensing platforms for the detection of pharmaceuticals in water samples.

Target	Functional monomer	Polymerisation method / Transducer	Electrochemical technique	Samples	Linear Range (nM)	LOD (nM)	Reference
Sulfamethoxazole	Py	Electropolymerisation, BDDE	SWV	Lake water	1.0×10^{2} – 1.0×10^{5}	24[a]	(Zhao *et al.*, 2015)
	MAA	Bulk polymerisation, SPCE, Fe_3O_4 MNPs	EIS	Seawater	0.1 – 1.0×10^{7}	1.0×10^{-3}[b]	(Zamora-Gálvez et al., 2016)
Sulfanilamide	Py	Electropolymerisation, PGE	DPV	Ground water	50 – 1.1×10^{3} 1.1×10^{3} – 4.8×10^{4}	20[c]	(Tadi *et al.*, 2014)
Azithromycin	4-ABA	Electropolymerisation, SPCE	DPV	River water and tap water	5.0×10^{2} – 1.0×10^{4}	80[d]	(Rebelo *et al.*, 2020)
Erythromycin	m-PD	Electropolymerisation, SPAuE	DPV	Tap water	2 – 16	0.1[b]	(Ayankojo *et al.*, 2020)
Chloramphenicol	DAM	Bulk polymerisation, MWCNTs, AuNPs, GCE	DPV	Seawater and reservoir water	0.31×10^{3} – 3.1×10^{5}	74[a]	(Zhao *et al.*, 2012)
Ciprofloxacin	MAA	Bulk polymerisation, Ch-AuNPs, GCE	DPV	Mineral and tap water	1.0×10^{3} – 1.0×10^{5}	2.1×10^{2}[e]	(Surya *et al.*, 2020)
Lomefloxacin	o-PD and β-CD	Electropolymerisation, Au electrode, Fe-PC	DPV	River and lake water	1 – 1.2×10^{2}	0.2[a]	(Li *et al.*, 2020b)
Chlortetracycline	o-PD	Electropolymerisation, GO, GCE	DPV	Tap water and laboratory wastewater	1.0×10^{4} – 5.0×10^{5}	Not mentioned	(Liu *et al.*, 2013)
Cefalexin	I3AA	Electropolymerisation, GCE, BDDE	DPV	River water	10 – 1.0×10^{3}	3.2 and 4.9[b]	(Feier *et al.*, 2019)
Mebendazole	MAA	Electropolymerisation, Fe-NCNF, GCE	DPV	Tap water and river water	10 – 1.5×10^{3}	4[a]	(Rao *et al.*, 2018)
17-β-estradiol	MNA	Electropolymerisation, PtNPs, GCE	DPV	Hospital wastewater and tap water	30 – 5.0×10^{4}	16[a]	(Yuan *et al.*, 2011)
	PATP	Electropolymerisation, AuNPs, Au electrode	LSV	River water	3.6×10^{-6} – 3.6	Not mentioned	(Florea *et al.*, 2015)
	An	Bulk polymerisation, Fe_3O_4 MNPs, SPCE	SWV	River water	50 – 1.0×10^{4}	20[a]	(Lahcen *et al.*, 2017)

[a] LOD calculated as S/N = 3.
[b] LOD calculated as 3 times the standard deviation of the blank divided by the slope.
[c] LOD calculated as 3.3 times the standard deviation of the blank divided by the sensitivity.
[d] LOD calculated as 3 times the standard deviation of the intercept divided by the slope.
[e] LOD formula no specified.

4-ABA: 4-aminobenzoic acid; β-CD: β-cyclodextrin; An: aniline; AuNPs: gold nanoparticles; BDDE: boron doped diamond; Ch-AuNPs: chitosan gold nanoparticles; DAM: diethylaminoethyl methacrylate; DPV: differential pulse voltammetry; EIS: electrochemical impedance spectroscopic; Fe-NCNF: nitrogen-doped carbon nanosheet frameworks decorated with Fe; Fe-PC: Fe doped porous carbon; GCE: glassy carbon electrode; GO: graphene oxide; I3AA: indole-3-acetic acid; LSV: linear sweep voltammetry; m-PD: m-phenylenediamine; MAA: methacrylic acid; MNA: 6-mercaptonicotinic acid; MNPs: magnetic nanoparticles; MWCNTs: multiwalled carbon nanotubes; o-PD: o-phenylenediamine; PATP: p-aminothiophenol; PGE: pencil graphite electrode; PtNPs: platinum nanoparticles; Py: pyrrole; SPAuE: screen printed gold electrode; SPCE: screen printed carbon electrode; SWV: square wave voltammetry.

Tetracycline antibiotics are highly prescribed worldwide because of their favourable properties both for human and animal therapy (Borghi and Palma, 2014; Li et al., 2020b; Van et al., 2020). More than 70% of these antibiotics are released in their active forms into the environment (Daghrir and Drogui, 2013; Javid et al., 2016) and, due its presence in waters, several studies have shown direct effects on microbial community structures (Grenni et al., 2018). Liu et al. (2013) developed a sensor to detect chlortetracycline (CTC), a derivate of tetracycline, based on electropolymerisation of o-PD and controlled electrochemical reduction of graphene oxide (GO) on a GCE. DPV measurements evaluated the electrochemical performance of the MIP-sensor for the analysis of tap water and a spiked laboratory wastewater sample. Although a current amplification effect and a higher electroconductivity through the electrochemical reduction of GO was expected, the sensor did not show a high sensitivity and the authors acknowledge the need to expand the linear concentration range ($1.0 \times 10^4 – 5.0 \times 10^5$ nM).

Cefalexin (CFX) is a broad-spectrum antibiotic that belongs to the class of cephalosporins (Rahim et al., 2019). Cephalosporins have been found in different aqueous matrices and river sediments in which cefalexin is the most frequently detected compound (Ribeiro et al., 2018). Its ubiquitous presence in sewage and wastewater is correlated with human and livestock populations. An electrochemical MIP sensor for its determination was recently described by Feier et al. (2019). Two different electrodes, GCE and BDDE, were used to assess the performances of the MIP sensors. Indole-3-acetic acid (I3AA) was chosen as the functional monomer, not only because it can be electropolymerised in aqueous solution, but also because of its functional groups that can form strong interactions with CFX. The indirect quantification of CFX was carried out by using $[Fe(CN)_6]^{3-/4-}$ and DPV. The LOD obtained with the BDDE was lower, but its precision was worse compared to the GCE. As mentioned above for the MIP sensor proposed for SMX (Zhao et al., 2015), BDDE provided very attractive advantages which was confirmed in this work: a more pronounced surface imprinting process and, consequently, a better sensitivity was achieved. However, GCE offered a better reproducibility and showed to be the most reliable transducer. This MIP sensor was easy to prepare and was successfully applied to river water analysis.

3.1.2 Anthelmintic

Unlike the variety of MIP-sensors for antibiotic analysis, to the best of our acknowledge only one MIP-based sensor for the detection of anthelmintic pharmaceuticals has been reported. This sensor combined hybrid nanomaterials with a MIP prepared by electropolymerisation for the simultaneous determination of mebendazole (MB) and catechol (Rao et al., 2018). A carbon nanosheet was created through a chemical blowing process on a GCE (Fig. 3B) and after electrochemical polymerisation of MAA with MB, it was observed that, due to their thin shells, nitrogen-doped carbon nanosheet frameworks decorated with Fe (Fe–NCNF) played a significant role in absorbing more MB molecules. Consequently, its frame structure with a large specific surface area allowed a good electron-transfer for the oxidation of MB at 0.82 V, but also supported the strong adsorption of catechol, which was electrochemically oxidised at 0.15 V. An easy-to-prepare and efficient MB sensor was obtained in this work. Fe–NCNF was synthetized using a simple process and its combination with a MIP, synthesized through electropolymerisation, amplified the electrochemical response of the sensor.

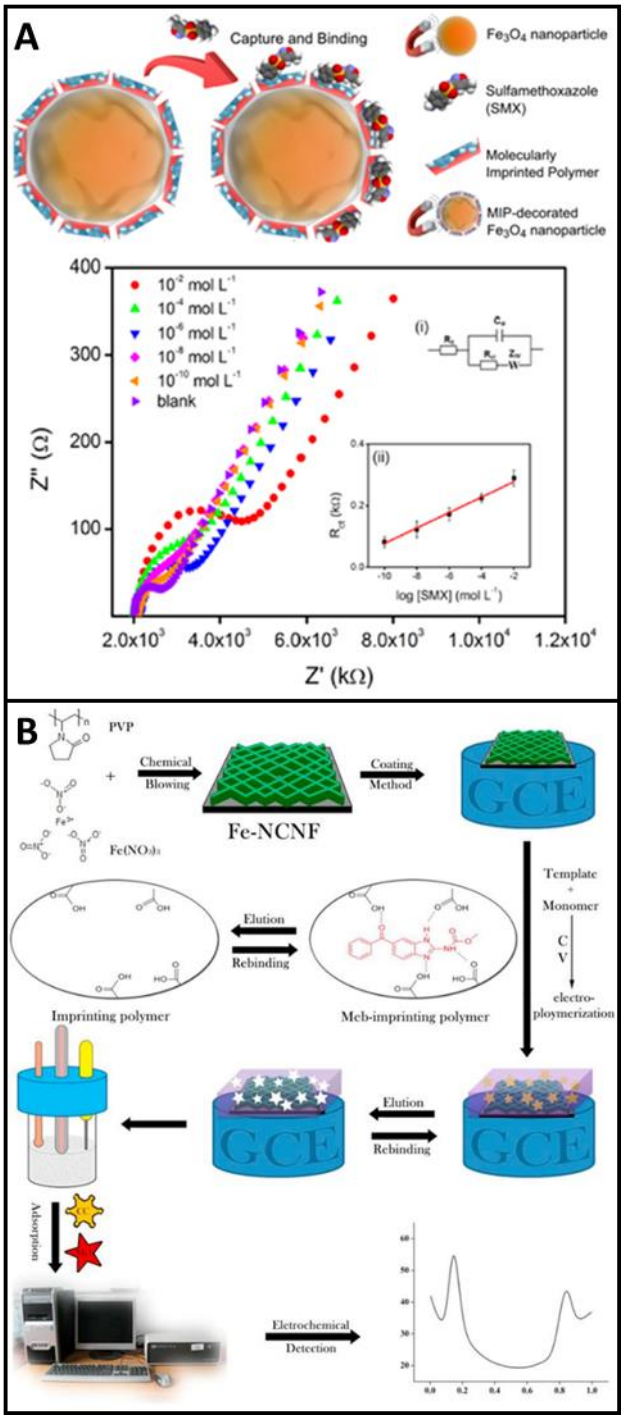

Figure 3. A) Schematic representation of the MIP-based sensor for SMX detection based on MIP-modified Fe3O4 MNPs and the Nyquist plots and calibration curve for the determination of SMX. Reproduced and adapted with permission from Zamora-Gálvez et al. (2016). Copyright 2016 American Chemical Society. B) Preparation and analysis procedures of the Fe–NCNF/MIP/GCE for detection of MB. Reproduced from Rao et al. (2018) with permission from Elsevier.

3.1.3 Hormones

Other substances present in environmental waters at concentrations of toxicological and carcinogenic concern are hormones, especially 17- β-estradiol (E2). E2 is commonly used in contraceptive pills and its release in water has gained notable attention, mainly because it is considered the major contributor to endocrine disruption of many species in the ecosystem (Salste et al., 2007). Additionally, it has been linked with breast cancer in women and prostate cancer in man (Adeel et al., 2017). E2 was also added to the EU Watch list of emerging aquatic contaminants (Decision, 2018/840/EU), highlighting the importance of

developing sensitive and accurate methods for its determination. In 2011, Yuan et al. (2011) reported an electrochemical MIP-based sensor for E2 quantification using a GCE modified with platinum nanoparticles (PtNPs). The MIP for E2 was constructed through the electropolymerisation of 6-mercaptonitic acid (MNA) and DPV was applied to directly detect the E2 binding to the MIP since it is an electroactive species. This sensor reached an LOD of 16 nM and was successfully applied to spiked hospital wastewater and tap water analysis. Later, Florea et al. (2015) developed another MIP sensor able to detect E2 via electropolymerisation of PATP. Assembled AuNPs on the surface of an Au electrode were used as electron wire for signal amplification, but in this work the response of the MIP sensor to E2 was measured indirectly by LSV. The combination of Fe_3O_4 with molecularly imprinting again showed to be an excellent tool for the highly specific detection of E2 (Lahcen et al., 2017). Lahcen et al. (2017) developed a Fe_3O_4-MIP sensing system with high selectivity towards E2 for the analysis of river water samples. Following the traditional bulk polymerisation strategy, MIP-modified Fe3O4 MNPs were obtained and then used to modify the working electrode surface of SPCE by drop-casting, leading to the enhancement of the direct oxidation current obtained by SWV. The developed sensor achieved an LOD of 20 nM.

3.2. Pesticides

Over the past 50 years, global sales of pesticides have increased because their importance in agricultural production. They inhibit and prevent the growth of harmful animals, insects, invasive plants, weeds, and fungi. However, repeated applications result in their accumulation in soils and they can be transported to the aquatic environment by surface runoff (Rousis et al., 2017). Considering their chemical properties and persistence, the biodiversity and the ecosystems' health is jeopardised since their toxic action is not restricted to target pests (Carvalho, 2017). Among all available pesticides, herbicides, insecticides, and fungicides are the most used types. Although electrochemical detection of pharmaceuticals in water samples using MIPs appears an unexplored area, many publications have been reported about their use for the trace analysis of pesticides, which are summarised in Table 2.

3.2.1 Insecticides

Organophosphates persist for days/weeks in the aquatic environment and studies showed that they are accumulated by crustaceans and fishes (Carvalho, 2017). These are the insecticides for which most electrochemical MIP sensors have been developed. As shown in Table 2 different strategies were adopted for the detection of chlorpyrifos (CPF) and the use of GCE is common to all of them. Xie et al. (2010b) reported a molecular self-assembly strategy for electropolymerisation of PATP on the surface of AuNPs-modified GCE by the formation of Au–S bonds. A linear range between 5.0×10^2 nM and 1.0×10^4 nM and an LOD of 330 nM were obtained. This sensor showed good interclass selectivity and the authors tested its applicability in spiked tap water. A better LOD (4.08 nM), was attained via simple bulk polymerisation of MAA (Xu et al., 2017). A GCE was coated with a suspension of the resulting MIP and the binding of CPF was evaluated by DPV using $[Fe(CN)_6]^{3-/4-}$ as redox probe. This simple sensor provided a good selectivity and its applicability was assessed in river water samples. However, an electrochemical MIP-sensor based on carbon nitride nanotubes (C3N4 NTs) decorated with graphene quantum dots (GQDs) (Yola and Atar, 2017) provided a much lower LOD (2.0×10^{-3} nM) in comparison with the previous works. As mentioned above, these nanomaterials have attracted great attention, and this work is one of the first reports that combines MIP with their excellent properties for application in wastewater samples. After the synthesis of the C3N4 NTs@GQDs composite by hydrothermal treatment, a suspension of this nanohybrid material was dropped onto the GCE surface. The electropolymerisation was performed using Py as functional monomer creating electrostatic interactions and hydrogen bonds with CPF. The performance of the prepared MIP sensor was evaluated directly by SWV. High conductivity of the electrode surface was achieved, and it was demonstrated that the introduction of a finite bandgap into graphene improved its gapless nature, showing the potential role of GQDs in the development of electrochemical sensors.

In another example of the use of nanomaterials, electrochemical MIP sensors for the analysis of methyl-parathion (MP) were prepared using both electro- and bulk polymerisation. Wu et al. (2014) constructed a sensor based on AuNPs decorated with CNTs. After electrodeposition of functionalised AuNPs on a

MWCNTs/GCE surface, the electrode was immersed in a solution containing PATP. Since MP is electroactive, its recognition by the MIP could be directly monitored by LSV. The proposed sensor allowed a low LOD (0.30 nM) and was successfully applied to the determination of MP in spiked distilled and tap water, and apple and cucumber samples with recoveries ranging from 95 to 106%.

Another quantitative method for MP was based on nitrogen-doped graphene sheets (N-GS) and a MIP synthetized by electropolymerisation of Ph (Xue et al., 2014). Although N-GS has been described as an excellent sensing material for molecular imprinting, the developed MIP-sensor showed a worse analytical performance than the one described above (Wu et al., 2014) (see Table 2).

The use of carbon paste-based electrodes (CPE) has some benefits that include easy surface modification and very low ohmic resistance (Toro et al., 2015; Vytras et al., 2009). These advantages were used to construct MIP sensors for parathion (Alizadeh, 2009) and diazinon (Motaharian et al., 2016), where the MIPs were synthetized by bulk polymerisation using MAA as functional monomer. The detection of these organophosphorus pesticides was performed by SWV and the authors demonstrated that the optimisation of the composition of the CPE is very important to improve the sensor's sensitivity.

The introduction of nanomaterials into CPEs seems to be crucial to achieve the best performance. In the past few years the rapid growth of research interest in metal organic frameworks (MOFs) linked via the self-assembly of transition metal ions/clusters and organic ligands has been observed (Xu et al., 2020b). Very recently, Xu et al. (2020b) based on its favourable characteristics like highly ordered structure and exposed sites, prepared a novel disposable carbon paste microelectrode (CPME) MIP sensor on zirconium (Zr) based MOF (UiO-66) to detect phosalone (PAS). UiO-66 was combined with Pt nanoparticles and the MIP imprinted with PAS was produced by the sol-gel method with 3-aminopropyltriethoxysilane (APTES) as the functional monomer. The resulting sensor exhibited an LOD of 0.078 nM and its feasibility was evaluated in lake water and soil samples.

Cypermethrin (CYP) belongs to the class of pyrethroid insecticides and its insecticidal action is more effective and less toxic compared to the organophosphates. So, this pesticide has been widely used through the world. Recently, a MIP-based sensor to determine CYP in spiked wastewater samples was reported (Atar and Yola, 2018). The sensing phase of the sensor was constructed on the surface of core-shell type nanoparticles (Fe@AuNPs) incorporating two-dimensional hexagonal boron nitride (2D-hBN) nanosheets through polymerisation of Ph. The highly sensitive properties of the prepared nanocomposite allowed a superior ability of specifically binding CYP and an extraordinary LOD (3.0×10^{-5} nM).

More recently, based on studies which showed a better performance of MIPs prepared with two or more functional monomers, Li et al. (2019d) produced a dual-monomer MIP for the analysis of CYP. Here, the preparation of the MIP sensor involved specific steps to produce a hybrid material by combining Ag and N co-doped zinc oxide (Ag–N@ZnO) with activated carbon (AC) (Fig. 4A). To produce an enlarged sensing surface and, consequently, amplify the signal, AC was chosen as a sensitising material on a GCE surface due to its low cost and easy availability. However, the authors reveal that the sole use of AC hinders the formation of a rigid layer on the electrode surface. This drawback was overcome by the addition of ZnO for better immobilisation. ZnO can easily be combined with other materials and doping can enhance its electrical conductivity. Therefore, as can be seen in Fig. 4A, Ag–N@ZnO was firstly produced by the sol-gel method and was then ultrasonically mixed with AC. After that, a suspension of the prepared solution was dropped on the GCE surface and the MIP was electropolymerised with dopamine (DA) and resorcinol (RC) as dual functional monomers. The electrochemical performance was evaluated by CV using $[Fe(CN)_6]^{3-/4-}$ as redox probe and the sensor was applied not only to water samples, but also to a soil sample. Although this dual monomer MIP provided a novel strategy to enhance binding and affinity with target analytes, the LOD was not as low as the MIP sensor proposed by Atar and Yola (2018), in which only one functional monomer was used.

Electrochemiluminescence (ECL) combined with MIPs can improve the sensitivity and selectivity of the assay. The use of ECL has seen an exponential growth in electrochemical sensors. However, the use of ECL as detection technique for MIP sensors with applications in real water samples is still scarce. An example of this combination is the sensor developed by Xu et al. (2020a) to detect the insecticide cyfluthrin (CYF). They developed a MIP platform based on QDs as luminophore in the presence of H_2O_2 as co-reactant. In the ELC process, both the luminophore and the co-reactant are oxidised or reduced at the electrode forming radical species. Then, an electrochemical reaction between their redox products occurs and radiation is emitted. Due to its high emission quantum yield, luminol is a classic ECL luminophore. However, an increase in the

demand of other alternatives has been observed because of limitations during its ECL process Li et al. (2019a).So, in the work developed by Xu et al. (2020a), the combination of a MIP with ECL based on QDs demonstrated high selectivity, good stability and controllability, where MWCNTs were utilised to improve the electrocatalytic activity and minimise surface fouling on the GCE. To simplify the electrode preparation process and improve the electrocatalytic activity, MIP-QDs were firstly synthetized by the sol-gel method using APTES as functional monomer. Then, the resulting MIP-QDs were used to coat the surface of a GCE (Fig. 4B). After drying, MWCNTs prepared in a Nafion solution, which can facilitate the adhesion and the ionic transportation across the electrode, were placed on the GCE surface. In the presence of CYF, the ECL and the redox peak current intensity decreased, which was accompanied by the increase of the electron transfer resistance. The LOD was 0.12 nM and good recoveries in seawater samples were obtained.

Table 2. Electrochemical MIP sensors constructed on different sensing platforms for the detection of pesticides in water samples.

Target	Functional monomer	Polymerisation method / Transducer	Electrochemical techniques	Samples	Linear Range (nM)	LOD (nM)	Reference
Chlorpyrifos	PATP	Electropolymerisation, GCE, AuNPs	CV	Tap water	5.0×10^{2} – 1.0×10^{4}	3.3×10^{2}[a]	(Xie et al., 2010b)
	MAA	Bulk polymerisation, GCE	DPV	River water	0.1 – 1.0×10^{4}	4.1[b]	(Xu et al., 2017)
	Py	Electropolymerisation, GCE, C_3N_4 NTs, GQDs	SWV	Industrial wastewater	1.0×10^{-2} – 1	2.0×10^{-3}[c]	(Yola and Atar, 2017)
Methyl-parathion	PATP	Electropolymerisation, GCE, AuNPs, CNTs	LSSV	Distilled water and tap water	0.38 – 4.2 4.2 – 42	0.30[a]	(Wu et al., 2014)
	Ph	Electropolymerisation, SPAuE, N-GS	CV	River water	3.8×10^{2} – 3.8×10^{4}	38[d]	(Xue et al., 2014)
Parathion	MAA	Bulk polymerisation, CPE	SWV	Tap, river and lake water	1.7 – 9.0×10^{2}	0.5[d]	(Alizadeh, 2009)
Diazinon	MAA	Bulk polymerisation, CPE	SWV	Well water	2.5 – 1.0×10^{2} 1.0×10^{2} – 2.0×10^{3}	0.79[b]	(Motaharian et al., 2016)
	MAA	Bulk polymerisation, CPE, MWNTs	SWV	Tap and river water	0.5 – 1.0×10^{3}	0.13[b]	(Khadem et al., 2017)
Phosalone	APTES	Sol-gel method, CPME, Pt-UiO-66	SWV	Lake water and soil	0.50–2.0×10^{4}	0.078[b]	(Xu et al., 2020b)
Cypermethrin	Ph	Electropolymerisation, GCE, Fe@AuNPs, 2D-hBN	DPV	Wastewater	1.0×10^{-3} – 10	3.0×10^{-5}[d]	(Atar and Yola, 2018)
	DA and RC	Electropolymerisation, GCE, Ag-N@ZnO, CHAC	EIS	Tap water and soil	2.0×10^{-4} – 8	6.7×10^{-5}[e]	(Li et al., 2019d)
Cyfluthrin	APTES	Sol-gel method, QDs, Nafion-MWCNTs	ECL	Seawater	0.46 – 2.3×10^{2}	0.12[a]	(Xu et al., 2020b)
Triazophos	PATP	Electropolymerisation, Au-electrode, luminol	ECL	Tap water, reservoir water and river water	0.1 – 1.0×10^{3}	0.058[d]	(Li et al., 2019a)
Glyphosate	Py	Electropolymerisation, Au-electrode	DPV	Tap water	30 – 4.7×10^{3}	1.6[b]	(Zhang et al., 2017)
	MAC	Bulk polymerisation, PGE, AuNPs, MWCNTs	DPASV	Soil	49 – 4.7×10^{2}	2.1[f]	(Prasad et al., 2014)

	PATP	Electropolymerisation, Au-electrode, AuNPs	LSV	Tap water	5.9×10^{-6} – 5.9	4.7×10^{-6}[a]	(Do et al., 2015)
2,4-dichlorophenol	MAA	Bulk polymerisation, GCE, microgel suspension, Ch, Nafion	DPV	Tap, river and drinking water	5.0×10^{3} – 1.0×10^{5}	1.6×10^{3}[e]	(Zhang et al., 2013)
	MAA	Bulk polymerisation, GCE, GO	DPV	Lake water	4 – 1.0×10^{4}	0.5[g]	(Liang et al., 2017)
	EDOT	Electropolymerisation, CFP	DPV	Lake, river and tap water	0.21 – 3.0×10^{2}	0.07[g]	(Maria G.C. et al., 2020)
4-Chlorophenol	o-PD	Electropolymerisation, GCE, ZnO NPs	SWV	Wastewater	2.0×10^{2} – 1.7×10^{5}	40[d]	(AL-Ammari et al., 2019)
Atrazine	Ph	Electropolymerisation, GCE, PtNPs, C_3N_4 NTs	SWV	Wastewater	1.0×10^{-3} – 1.0×10^{-1}	1.5×10^{-4}[d]	(Yola and Atar, 2017)
2,4-Dichlorophenoxy acetic acid	Py	Electropolymerisation, GCE	CV	Tap water	1.0×10^{-3} – 1.0×10^{4}	8.3×10^{2}[a]	(Xie et al., 2010a)
Paraquat	Py	Electropolymerisation, PGE, EBB	DPV	Dam water	5.0×10^{3} – 5.0×10^{4}	2.2×10^{2}[a]	(Sayyahmanesh et al., 2016)
Diuron	MAA	Bulk polymerisation, CPE, MWCNTs	SWV	River water	52 – 1.3×10^{3}	9.0[b]	(Wong et al., 2015)
Chloridazon	2-VP and MAA	Bulk polymerisation, CPE, MWCNTs	DPV	Ground, surface, seawater and drinking water	5.0×10^{2} – 4.0×10^{5}	62[d]	(Ghorbani et al., 2020)
Hexazinone	2-VP	Bulk polymerisation, CPE	DPV	River water	0.019 – 0.11	2.6×10^{-3}[d]	(Toro et al., 2015)
Dicloran	MAA	Bulk polymerisation, CPE, MWCNTs	SWV	Tap water and river water	1.0×10^{3} – 1	0.48[d]	(Khadem et al., 2016)
Tributyltin	APTES	Sol-gel method, SPCE, Fe_3O_4 MNPs	EIS	Sea water	5.0×10^{-3} – 5.0×10^{3}	5.4×10^{-3}[g]	(Zamora-Gálvez et al., 2017)

[a] LOD calculated as 3 times the standard deviation of the blank.
[b] LOD calculated as 3 times the standard deviation of the blank divided by the slope.
[c] LOD calculated as 3.3 times the standard deviation of the intercept divided by the slope.
[d] LOD formula no specified.
[e] LOD calculated as S/N = 3.
[f] LOD based on the minimal distinguishable signal for lower concentration of analyte.
[g] LOD calculated as 3 times the standard deviation of the lowest concentration (or any concentration) divided by the slope.

2D-hBN: two dimensional hexagonal boron nitride; 2-VP: 2-vinylpyridine; APTES: (3-Aminopropyl)triethoxysilane; Ag-N@ZnO: silver and nitrogen co-doped zinc oxide; C_3N_4 NTs: carbon nitride nanotubes; CFP: carbon fiber paper; Ch: chitosan; CHAC: activated carbon prepared from coconut husk; CMPE: carbon paste microelectrode; CNTs: carbon nanotubes; CPE: carbon paste electrode; CV: cyclic voltammetry; DA: dopamine; DPASV: differential pulse anodic stripping voltammetry; EBB: eriochrome blue-black B; ECL: electrochemiluminescence; EDOT: 3,4-ethylenedioxythiophene; Fe@AuNPs: core-shell type nanoparticles; GQDs: graphene quantum dots; LSSV: linear stripping sweep voltammetry; MAC: N-methacryloyl-L-cysteine; N-Gs: nitrogen doped graphene sheets; Ph: phenol; Pt-UiO-66: Zr-based metal–organic framework catalyst; QDs: quantum dots; RC: resorcinol; ZnO NPs: zinc oxide nanoparticles.

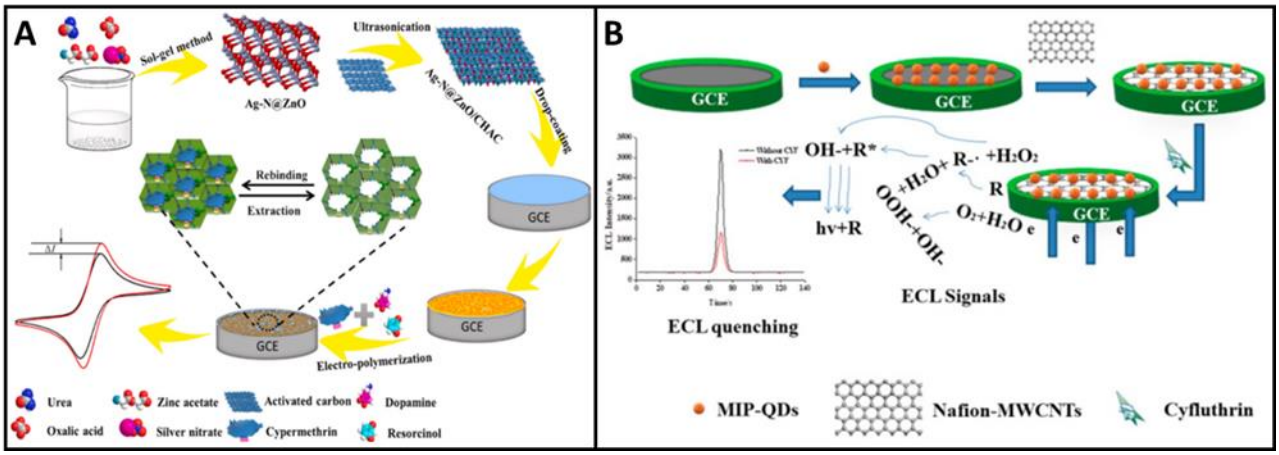

Figure 4. A) Schematic representation of the fabrication and characterisation of a dual MIP monomer based on Ag–N@ZnO/CHAC/GCE. Reproduced from Li et al. (2019d) with permission from Elsevier. B) Schematic representation of a MIP ECL sensor to detect CYF. Reproduced from Xu et al. (2020a).

3.2.2 Herbicides

Glyphosate (Gly) is among the mostly widely used herbicides by farmers during the past 40 years. Although not proven, Gly has been associated with cancer in humans and a strong debate about its potential harmfulness has been generated (Silva et al., 2018). Due to its persistence in seawater (Mercurio et al., 2014), the need to identify trace levels of Gly in drinking water is also urgent. To the best of our acknowledge, the most recent electrochemical MIP-sensor used for Gly detection in water samples was reported by Zhang et al. (2017). In this work, a simple electropolymerisation procedure, using Py as functional monomer, on an Au electrode was performed. The sensor presented good binding kinetics to Gly and showed good stability, selectivity, and sensitivity, and an LOD of 1.60 nM. The analytical signal was based on the use of the $[Fe(CN)_6]^{3-/4-}$ redox probe and DPV. This MIP sensor exhibited a higher sensitivity when compared with the MIP sensor constructed by Prasad et al. (2014), where N-methacryloyl-L-cysteine (MAC) molecules were used as monomer in the bulk polymerisation process. However, the best sensitivity to detect GLY in water samples was obtained by the construction of an electrochemical sensor based on MIP-MOF films formed on Au surfaces through electropolymerisation of PATP functionalised with AuNPs (Do et al., 2015). A low LOD of 4.7 × 10^{-6} nM was achieved and the sensing capacity of the sensor was evaluated in tap water.

All other published MIP-sensors to detect herbicides with applications in water samples were based on the modification of GCE (AL-Ammari et al., 2019; Liang et al., 2017; Xie et al., 2010a; Yola and Atar, 2017; Zhang et al., 2013), PGE (Sayyahmanesh et al., 2016) or CPE (Ghorbani et al., 2020; Khadem et al., 2017; Toro et al., 2015; Wong et al., 2015). Additionally, a newly developed carbon fibre paper used as working electrode was also reported (Maria et al., 2020). In order to enhance the selectivity and precision, various nanomaterials were combined in these sensors.

As can be seen in Table 2, the LOD for 2,4-dichlorophenol (2,4-DCP), a typical chlorophenol that is widely employed in the synthesis of herbicides and insecticides, was much lower in the presence of GO (Liang et al., 2017). Moreover, Liang et al. (2017), using the same functional monomer (MAA), proposed a very simple methodology for the fabrication of a 2,4-DCP-MIP electrochemical sensor in comparison with Zhang et al. (2013). Besides using MAA as functional monomer, Zhang et al. (2013) also used a co-monomer, chlorohemin, to introduce chemically active sites into the MIP as well as a combination of chitosan (Ch) and Nafion for immobilisation of the MIP and to increase conductivity, respectively. This assembly probably blocked the mass transport to the electrode surface which resulted in a worse LOD. More recently, one of the first reports using a poly(3,4-ethylenedioxythiophene) (PEDOT) based MIP on carbon fibre paper, and the first applied to water samples, was published by Maria et al. (2020). To detect 2,4-DCP, carbon fibre paper was chosen as working electrode because of its porosity, offering abundant reaction sites. This novelty and the use of PEDOT as conductive polymer not only improved the LOD (0.07 nM), but also the stability and reproducibility. Other

approach was presented by AL-Ammari et al. (2019), in this case, to explore the detection of 4-chlorophenol (4-CP). The MIP was prepared by electropolymerisation of o-PD with multifunctional nanomaterials, zinc oxide nanoparticles (ZnO NPs) and graphene platelets, on a GCE. Compared with other techniques applied for the detection of 4-CP, this MIP, which was tested in real wastewater samples, showed higher sensitivity. Another excellent approach to improve the LOD was based on combining Pt NPs and C_3N_4 NTs, which were obtained by hydrothermal treatment and allowed minimised waste formation. Yola and Atar (2017) employed these nanomaterials to modify a GCE surface and, through electropolymerisation of Ph, they created a sensor that showed an LOD of 1.5×10^{-4} nM for the analysis of atrazine (ATR). PATP was also investigated for the determination of 2,4-dichlorophenoxy acetic acid (2,4-D) (Xie et al., 2010a). In this work, a simple procedure which involved electropolymerisation on the surface of a GCE, was developed. The 2,4-D molecules were removed from the polymeric matrix without solvent extraction, which is in accordance with "green chemistry". However, this simple sensor did not show a great LOD.

Due to the favourable features of Py in aqueous media, it was chosen again as functional monomer for the recognition of paraquat in dam water (Sayyahmanesh et al., 2016). The electropolymerisation of the MIP occurred on top of a PGE in the presence of a functional doping ion (eriochrome blue-black B (EBB)). EBB is an anionic complexing agent, which was used to maintain the electroneutrality during the reduction of Py and, consequently, to conserve its electroactivity. In order to enhance the electrochemical signal of diuron, a CPE modified with a MIP and MWCNTs was proposed by Wong et al. (2015). The MIP was synthetized via bulk polymerisation. This polymerisation technique was also adopted by (Ghorbani et al., 2020) for the determination of chloridazon (CLZ) in surface, ground and drinking water. This MIP sensor was constructed based on the multiple interactions formed between CLZ and two functional monomers, 2-vinylpiridine (2-VP) and MAA. In the same way, but without the use of nanomaterials, Toro et al., 2015 developed a selective sensor for hexazinone (HXZ) using computational simulations to evaluate the interaction of HXZ with functional monomers in the prepolymerisation mixture. MAA was selected as the most suitable monomer and this computational study allowed the production of a more effective MIP for HXZ with an excellent LOD of 2.6×10^{-3} nM.

3.2.3 Fungicides and biocides

Compared with insecticides and herbicides, the number of publications on the analysis of fungicides is much lower (see Table 2). An electrochemical MIP-sensor for the determination of dicloran in tap water and river water was developed by Khadem et al. (2016). In this work, the MIP produced by bulk polymerisation was deposited on top of a CNTs-modified CPE. The sensor showed very high recognition ability in comparison with a NIP electrode with a linear range between 1 and 1.0×10^3 nM and an LOD of 0.48 nM.

Besides this, a MIP sensor for tributyltin (TBT), a biocide used in antifoulant paints to prevent the growth of marine organisms on the hulls of large ships, was also described (Zamora-Galvez et al., 2017). Fe_3O_4 MNPs were used to modify the MIP prepared by the sol-gel process using APTES as monomer. Using an SPCE as transducer and EIS as detection technique, a low LOD was achieved (5.4×10^{-3} nM).

3.3 Heavy metals

In developing countries, the increase of industrial activity and urbanisation has led to the proliferation of heavy metals in the soil and water sources (Ali et al., 2019a). The pollution of the environment with heavy metals has a particular impact on ecotoxicology because of their long persistence, non-degradability, bioaccumulation and biomagnification in the food chain, which causes serious harm not only to wildlife, but also to human health (Hong et al., 2020; Kumar et al., 2019). The MIP technology has attracted considerable attention to assess and monitor the concentration of heavy metals (Liu et al., 2019; Yaroshenko et al., 2020). In the field of separation and sensing, several works involving the adsorption of heavy metals using MIPs can be found in the literature (Sharma and Kandasubramanian, 2020). However, as shown in Table 3, only a small number of publications concerning electrochemical MIP-based sensors to detect metal ions with applications in water and soil samples were reported. Electrochemical MIP sensors for the analysis of beryllium(II) (Be^{2+}) (Li et al., 2015), cobalt(II) (Co^{2+}) (Li et al., 2019), copper(II) (Cu^{2+}) (Di Masi et al., 2020; Prasad and Fatma, 2016; Prasad and Singh, 2016) and zinc(II) (Zn^{2+}) (Shirzadmehr et al., 2016) were developed following different

strategies to facilitate metal ion imprinting and improve the selectivity of the sensor. The combination of MIP and ECL was reported for ultra-trace Be^{2+} detection in water samples (Li et al., 2015). The sensor was fabricated using Be^{2+} and 4-(2-pyridylazo)-resorcinol (PAR), a metallochromic indicator, to form a complex which was copolymerised with o-PD. CV characterisation of the prepared MIP sensor revealed that the imprinted cavities could only recognise the Be2+-PAR complex and not the metal ion and the ligand, showing an efficient imprinting process. ECL was indirectly measured by the luminol-H_2O_2 interaction and a low LOD (0.024 nM) was achieved. The same strategy for the detection of nanomolar levels of Co^{2+} was used by Li et al. (2019c). In their work, Co^{2+} and bovine serum albumin (BSA) were introduced as the template molecules and an ECL sensor was designed. Another attractive and different concept, based on biosorption, was described to detect Cu^{2+} in soil and water samples (Prasad and Fatma, 2016; Prasad and Singh, 2016). As certain algae show enormous potential for biosorption of heavy metals, Prasad and Fatma (2016) used a blue green-algae (*Aulospira* sp.) modified PGE for the development of one MoNomer Ion Imprinted Polymer (OMNiMIP) (Fig. 5A). In this procedure, the functionalised algae were simultaneously used as crosslinker and functional monomer. The use of carboxylic groups in the OMNiMIP sensor facilitated the metal ion imprinting and a highly sensitive method with precise results was obtained. The absence of an extra crosslinker allowed the LOD to be several times lower than the one obtained by Prasad and Singh (2016). In this work, the same algae were employed as a natural ligand to form a "complex-metal" with N-methacryloylglutamic acid (NMGA) as the monomer for the analysis of Cu^{2+}. The algae were considered as cheap substitutes of MWCNTs to impart electroconductivity to the film. Using differential pulse anodic stripping voltammetry (DPASV), an extremely sensitive technique used for the detection of heavy metal ions, Prasad and Singh (2016) developed a OMNiMIP without the need to select a crosslinker and, consequently, without optimisation of the monomer-crosslinker ratio.

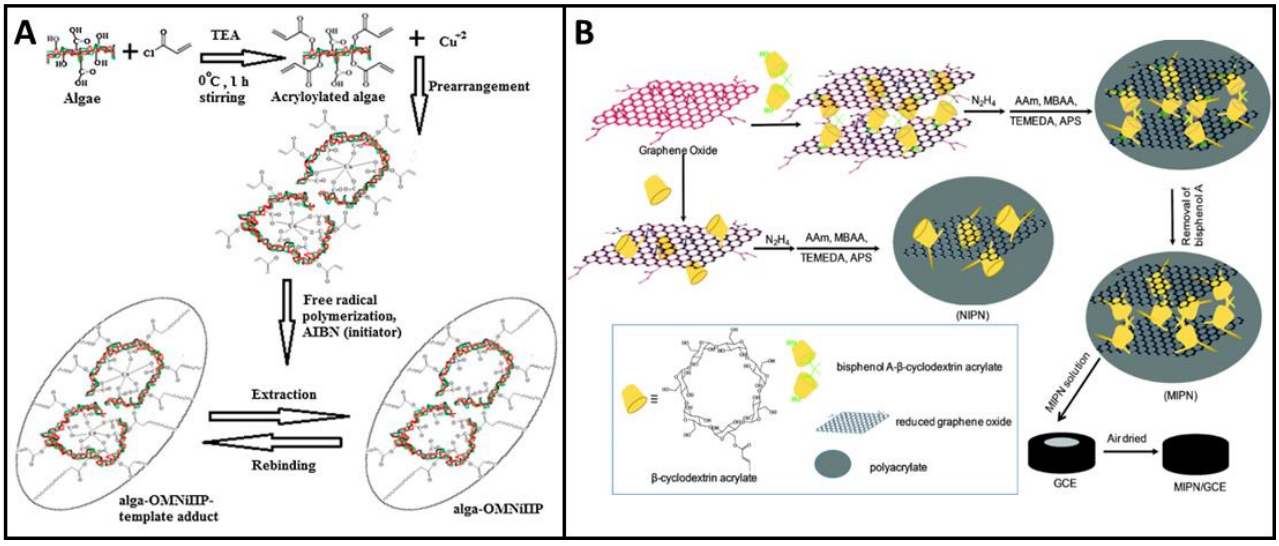

Figure 5. A) Illustration of the preparation of an alga-OMNiMIP for electrochemical detection of Cu^{2+}. Reproduced from Prasad and Fatma (2016) with permission from Elsevier. B) Schematic illustration of the synthesis procedure of a MIP sensor for BPA analysis. Reproduced from Ali et al. (2019b) with permission from the Centre National de la Recherche Scientifique (CNRS) and The Royal Society of Chemistry.

Table 3. Electrochemical MIP sensors constructed in different sensing platforms for detection of heavy metals in water samples.

Target	Functional monomer	Polymerisation method / Transducer	Electrochemical techniques	Samples	Linear Range (nM)	LOD (nM)	Reference
Beryllium(II) (Be^{2+})	o-PD	Electropolymerisation, SPAuE, luminol–H_2O_2	ECL	Rain, bottled and well water	0.07 – 8.0	0.024[a]	(Li *et al*., 2015)
Cobalt(II) (Co^{2+})	o-AP	Electropolymerisation, Au electrode, BSA, MWCNTs, Cu, C-Dots	ECL	Surface water, industrial sewage and agricultural soil	1 – 1.0×10^2	0.31[a]	(Li *et al*., 2019c)
Copper(II) (Cu^{2+})	Acryloylated-algae	Bulk polymerisation, PGE	DPASV	Lake water and soil	0.13 – 1.2×10^2	0.028[b]	(Prasad and Fatma, 2016)
	NMGA	Bulk polymerisation, PGE	DPASV	Lake water and soil	0.16 – 98	0.060[b]	(Prasad and Singh, 2016)
	o-PD	Electropolymerisation, SPPtE	DPV	Drinking water	0.95 – 2.4×10^2	2.7[c]	(Di Masi *et al*., 2020)
Zinc(II) (Zn^{2+})	MAA	Bulk polymerisation, CPE, GO, AgNPs, [BMP]Tf2N (IL)	Potentiometry	River water, industrial wastewater	3.9 – 1.0×10^{10}	0.030[d]	(Shirzadmehr et al., 2016)

[a] LOD calculated as 3 times the standard deviation of the intercept divided by the slope.
[b] LOD calculated as 3 times the standard deviation of the blank divided by the slope.
[c] LOD calculated as 3 times the standard error from the weighted regression plot divided by the slope.
[d] LOD formula no specified.

AgNPs: silver nanoparticles; [BMP]Tf2N (IL): ionic liquid 1-butyl-1-methylpyrrolidinium bis(trifluoromethylsulfonyl)imide; BSA: bovine serum albumin; C-Dots: carbon dots; NMGA: N-methacryloylglutamic acid; o-AP: o-aminophenol; SPPtE: screen printed platinum electrode.

3.4 Other contaminants

Besides pharmaceuticals, pesticides and heavy metals, the environment is also charged with other chemicals that may harm human health. Many products of daily use, such as industrial explosives, sub-products of industrial syntheses, ingredients of cosmetics, brominated flame retardants or even amino acids have not surprisingly been detected in environmental matrices. As can be observed in Table 4, a substantial amount of work has been done to develop novel sensors to determine the presence of these unwanted compounds in different environmental water samples. In this section, emphasis will only be given to new design strategies of MIPs.

Since 2011, bisphenol A (BPA) has attracted widespread attention as contaminant. It is mainly used to produce epoxy resins and polycarbonate plastics and is found in bottles, food containers and toys. BPA is considered an endocrine disruptor and human exposure leads to a variety of health issues (Ali et al., 2019b). Various electrochemical strategies have been used for the selective determination of BPA in different types of waters (Ali et al., 2019b; Chen et al., 2014b; Dadkhah et al., 2016; Tan et al., 2016; Wang et al., 2011; Zhu et al., 2014) (see Table 4). There is no consensus on the technique used for its molecular imprinting, but the presence of nanomaterials was essential for the adequate performance of the sensors. Recently, Ali et al. (2019b) reported a very robust MIP based on a nanocomposite of polyacrylate, reduced GO (rGO) and β-cyclodextrin that were covalently linked forming a 3D network (Fig. 5B). β-cyclodextrin is known to form an inclusion complex with BPA by means of host-guest complexation, while polyacrylate allows to form porous 3D networks. The first step of the synthesis consisted of the reaction between GO and β-cyclodextrin in the presence of BPA; the hydroxyl groups of β-cyclodextrin strongly react with the epoxide groups of GO and a stable interaction is obtained. Then, radical polymerisation was performed using two functional monomers, acrylamide (AA) and N,N' -methylenebis-acrylamide (MBAA). The electrochemical detection of BPA was performed using GCE as transducer, reaching an interesting LOD (8 nM). In this work the combination of rGO

and β-cyclodextrin in molecular imprinting was explored for the first time, providing promising insights for the design of more selective MIPs.

The same LOD was observed with a low-cost imprinted sensor based on laser scribed graphene (LSG) technology (Beduk et al., 2020). This device was used as transducer to detect BPA after electropolymerisation of Py. Dadkhah et al. (2016) and Wang et al. (2011) developed strategies to prepare MIPs on the surface of GO and hexagonally structured mesoporous silica, respectively, to enhance the electrochemical signal. In both works, amine functionalisation of GO and SiO_2 NPs was achieved by a simple procedure using APTES to improve the recognition ability of the sensors. After functionalisation, the targets were immobilised on its surface and not only many homogenous imprinting sites were formed, but also an easy access of the analyte molecules to the imprinting sites was reported. At the same time, the best LOD found for BPA was 3 nM using GO in the modification of the electrochemical MIP sensor. Recently, ECL again showed its potential to achieve a higher sensitivity (Zhang et al., 2020). These authors developed a MIP sensor based on a GCE modified with Fe_3O_4 nanocrystals (Fe_3O_4–NCs), which increased the ECL response signal of luminol. The proposed MIP sensor displayed an excellent analytical performance and a low LOD (1.8×10^{-3} nM) was observed.

Another compound that is widely used in epoxy and polycarbonate resins is tetrabromobisphenol A (TBBPA), which is the most common brominated flame retardant on the market (Zhou et al., 2016). TBBPA has also been linked with endocrine disruption. For its electrochemical detection, Chen et al. (2014a) presented a MIP based on nickel nanoparticle-modified GO and showed that the combination of more than one nanostructured material increased the effective surface that can be an attractive route for the preparation of MIP-based sensors with adequate sensitivities.

Table 4. Electrochemical MIP sensors constructed on different sensing platforms for the detection of various contaminants in water samples.

Target	Functional monomer	Polymerisation method / Transducer	Electrochemical techniques	Samples	Linear range (nM)	LOD (nM)	Reference
2,4,6-Trinitrotoluene	MAA	Bulk polymerisation, CPE	SWV	Tap water, ground water and soil	$5 - 1.0\times10^3$	1.5[a] 5[a]	(Alizadeh *et al*., 2010)
	MAA	Bulk polymerisation, CPE, Fe_3O_4 MNPs	SWV	Tap and sea water	$1.0 - 1.3\times10^1$	0.5[a]	(Alizadeh, 2014)
Bisphenol A	MMA	Miniemulsion polymerisation, CPE, Fe_3O_4 MNPs, CTAB	EIS	Drinking bottle and lake water	$6.0\times10^2 - 1.0\times10^5$	1.0×10^2[a]	(Zhu *et al*., 2014)
	4-VP	Bulk polymerisation, CPE, MWCNTs	DPV	River, tap and pure water	$80 - 1.0\times10^5$	22[b]	(Chen *et al*., 2014b)
	AA and MBAA	Bulk polymerisation, GCE, β-CD, GO	DPV	Lake, tap and drinking water	$20 - 1.0\times10^3$	8[c]	(Haydar Ali et al., 2019)
	Py	Electropolymerisation, GCE, GQDs	DPV	Tap and sea water	$1.0\times10^2 - 5.0\times10^4$	40[a]	(Tan *et al*., 2016)
	Py	Electropolymerisation, LSG electrode	DPV	Mineral and tap water	$50 - 2.0\times10^4$	8[a]	(Beduk et al., 2020)
	APTES	Sol-gel method, GCE, GO	DPV	Mineral water	$6 - 1.0\times10^2$ $2.0\times10^2 - 2.0\times10^4$	3[b]	(Dadkhah *et al*., 2016)
	APTES	Sol-gel method, CPE, SiO_2 NPs	CV	River water	$1.0\times10^2 - 5.0\times10^5$	32[c]	(Wang *et al*., 2011)
	APTES	Sol-gel method, GCE, Fe_3O_4-NCs	ECL	Seawater	$8.8\times10^{-3} - 2.2\times10^4$	1.8×10^{-3}[d]	(Zhang *et al*., 2020)

Tetrabromobisphenol A	Py	Electropolymerisation, GCE, GO, NiNPs	DPV	Tap water, rain and lake water	0.5 – 1.0×10^4	0.13[a]	(Chen *et al.*, 2014a)
	APTES	Sol-gel method, CPE, Fe_3O_4 MNPs	DPV	Tap water, rain and pool water	5.0 – 2.0×10^3	0.77[b]	(Zhou *et al.*, 2016)
Tetrabromobisphenol S	MAA and PATP	Bulk polymerisation, CPE, AuNPs	DPV	Tap, lake and drinking water	0.1 – 10	0.029[b]	(Sarpong *et al.*, 2020)
Sodium Lauryl sulfate	2-ATP	Electropolymerisation, SPAuE	DVP	Wastewater and river water	0.1 – 3.5	6.3×10^{-4}[b]	(Motia *et al.*, 2018)
3-Methylindole	o-PD	Electropolymerisation, GCE	CV	Tap and lake water	10 – 1.2×10^3	4[d]	(Yu *et al.*, 2019)
4-nonylphenol	Py	Electropolymerisation, GCE, GO	DPV	Rain and lake water	0.45 – 45	0.016[a]	(Chen *et al.*, 2013)
Para-nitrophenol	MAA	Bulk polymerisation, CPE	DPV	River and tap water	8 – 5.0×10^3	3[c]	(Alizadeha et al., 2009)
N-Nitrosodimethylamine	Py	Electropolymerisation, GCE, SWCNTs	EIS	Bottled drinking water and tap water	1.4×10^2 – 3.1×10^3	11.5[d]	(Cetó *et al.*, 2016)
L-cystein	MAA	Bulk polymerisation, CPE	DPV	Tap water	20 – 1.8×10^2	9.6[a]	(Aswini *et al.*, 2014)
Triclosan	AA	Bulk polymerisation, SPAuE, PVC-COOH	DPV	Wastewater and mineral water	3.5×10^{-4} – 3.5×10^2	7.9×10^{-4}[d]	(Motia *et al.*, 2019)
Methyl green dye	AA	Bulk polymerisation, CPE, Fe_3O_4	SWAdASV	River water and industrial wastewater	99 – 1.8×10^3	10[c]	(Khan *et al.*, 2019)
Diphenylamine	([VC4mim][PF6] (IL)	Bulk polymerisation, GCE, RGO, Fe_3O_4	DPV	Lake water	1.0×10^2 – 1.8×10^3	50[a]	(Liu *et al.*, 2018)

[a] LOD calculated as S/N = 3.
[b] LOD calculated as 3 times the standard deviation of the blank divided by the slope.
[c] LOD formula no specified.
[d] LOD calculated as 3 times the standard deviation of the blank.

2-ATP: 2-aminothiophenol; 4-VP: 4-vinylpyridine; AA: acrylamide; CTAB: Cetyltrimethylammonium bromide; MBAA: N,N'-methylenebis-acrylamide; NCs: nanocrystals; NiNPs: nickel nanoparticles; LSG: laser scribed graphene; PVC-COOH: carboxylic polyvinyl chloride; RGO: reduced Graphene oxide; SiO_2 NPs: silica nanoparticles; SWAdAS: square-wave adsorptive anodic stripping; SWCNTs: single walled carbon nanotubes; ([VC4mim][PF6] (IL): ionic liquid 1-vinyl-3-butylimidazolium hexafluorophosphate.

Incorporation of ionic liquids (ILs) in the MIP framework has also been the focus of many studies. By exploring their good electrocatalytic activity, adsorption capacity and multiple interactions with targets, there are some works adopting polymerisable ILs as functional monomers and crosslinkers to prepare MIPs (Ding et al., 2020). Liu et al. (2018) introduced a new IL composite using IL 1-vinyl-3-butylimidazolium hexafluorophosphate ([VC4mim][PF6]) as functional monomer, IL 1,4-butanediyl-3,3' -bis-l-vinylimidazolium dihexafluorophosphate ([V2C4(mim)2][(PF6)2]) as crosslinker and GO and Fe3O4 as support, to detect diphenylamine (DPA) in water samples. In their work the authors showed that the proposed MIP based on such IL as crosslinker had a higher electrochemical response than that of the traditional ethylene glycol dimethacrylate. Although, ILs have been considered alternative green solvents, it is important to note that ILs are quite expensive and their recycling is difficult.

Another strategy in surface imprinting was shown by Motia et al. (2019) through the functionalisation of an SPAuE with a carboxylic polyvinyl chloride (PVC–COOH) layer for the detection of triclosan (TCS), which is an antibacterial agent incorporated in many products of daily use. After linking TCS with PVC, strong hydrogen bonds between the polar groups of TCS and –COOH groups of the PVC were established.

4. Conclusions and perspectives

Environmental water quality monitoring is essential to ensure the safety of the aquatic environment and, consequently, human and animal health. Moreover, the analysis of contaminants in the environment is essential to know their pathways, fate and effects, but also to determine the WWTP's removal efficiency.

In this review, the considered studies demonstrated a significant increase in the development of MIP-based electrochemical sensors to detect contaminants in water samples. MIPs are polyvalent receptors, which are easily synthetized, modified and manipulated and, more importantly, they are compatible with water. The MIP's sensitivity and affinity are usually improved by their combination with nanomaterials. This has stimulated researchers to design and create new and innovate MIP sensors with the ability to recognise the target molecules at trace levels. However, although MIPs have proven their potential as recognition elements, the need of extremely low LODs remains an open challenge. This is the reason why many MIP sensors for determination of pharmaceuticals are not applied to water analysis but to serum and/or urine (for clinical control) or pharmaceutical formulations (for quality control).

Regarding the imprinting process, there is no specific approach for a particular class of molecules. So, the synthesis process and functional monomer that provide the best MIP for the target molecule have to be obtained by experimental studies. In this context, computational studies, reported only in few publications, are increasingly used since they have proven to be valuable for selecting suitable functional monomers. Besides the fact that computational modelling allows a better understanding of the monomer-template interactions, it provides important guidelines and, therefore, leads to an overall more environmentally friendly process for MIP construction. Accordingly, more efforts should be made to exploit theoretical approaches to pre-screen the preparation conditions, since good selectivities and LODs are achieved. Regarding the transducers, carbon electrodes are undoubtedly the most widely reported sensing platform for the determination of contaminants. Regarding the detection strategy, the highest sensitivity is usually attained by indirect electrochemical sensing, although this strategy can have some drawbacks, such as false results due to the presence of masked interferents.

Although MIPs are highly selective, this can also be a disadvantage when the determination of several contaminants is required. Thus, the development of MIPs capable to recognise more than one contaminant (for example, a family of contaminants with similar molecular structures) could be useful for some applications. Another approach could be the development of multiplex MIP-based sensors, although nowadays they are scarce for environmental applications. Moreover, portable electrochemical sensors show another difficulty for their application in environmental analysis: analytes have to be extracted from solid samples (such as soils) to allow analysis. Liquid samples, mainly water, are easier to analyse (since they are aqueous); however, sometimes they present a complex matrix that could interfere in the analysis.

Therefore, continuous studies within multidisciplinary teams must be performed to develop highly sensitive and accurate methods, aiming to implement MIPs in the analysis of contaminants in environmental waters. The construction of portable MIP sensors, especially by using screen printed electrodes, could be very useful in field applications. However, the commercialisation of these sensors remains a challenge, since, as for other kind of sensors (biological sensors and sensors for food applications), the knowledge transfer from laboratories to the market is difficult.

Acknowledgements

The authors are grateful for the financial support from the Fundação para a Ciência e a Tecnologia (FCT) / the Ministério da Ciência, Tecnologia e Ensino Superior (MCTES) through national funds (Portugal) (UIDB/50006/2020 and UIDP/50006/2020). The authors would also like to thank to the EU and FCT / UEFISCDI

/ FORMAS for funding in the frame of the collaborative international consortium REWATER, financed under the ERA-NET Cofund WaterWorks 2015 Call. This ERA-NET is an integral part of the 2016 Joint Activities developed by the Water Challenges for a Changing World Joint Programme Initiative (Water JPI). This work was also supported by the project Farmasense (39957), funded by Sistema de Incentivos à Investigação e Desenvolvimento Tecnológico de Portugal 2020, through the Programa Operacional do Norte (NORTE 2020) and the Fundo Europeu de Desenvolvimento Regional (FEDER). Isabel Seguro received her research Grant through this project. E. Costa-Rama thanks the Government of Principado de Asturias and Marie Curie-Cofund Actions for the post-doctoral grant "Clarín-Cofund" (ACA17-20). Patrícia Rebelo is grateful to FCT for her PhD grant (SFRH/BD/132384/2017). João Pacheco is grateful to FCT for his postdoc grant (SFRH/BPD/101419/2014), financed by POPH-QREN-Tipologia 4.1-Formação Avançada, funded by Fundo Social Europeu and MCTES.

References

Adeel, M., Song, X., Wang, Y., Francis, D., Yang, Y., 2017. Environ. Int. 99, 107–119.
Adumitrăchioaie, A., Tertiș, M., Cernat, A., Săndulescu, R., Cristea, C., 2018. Int. J. Electrochem. Sci. 13, 2556–2576.
Afonso-Olivares, C., Sosa-Ferrera, Z., Santana-Rodríguez, J.J., 2017.. Sci. Total Environ. 599–600, 934–943.
Ahmad, O.S., Bedwell, T.S., Esen, C., Garcia-cruz, A., Piletsky, A., Le, L., 2019. Trends Biotechnol. 37, 294–309.
AL-Ammari, R.H., Ganash, A.A., Salam, M.A., 2019. Synth. Met. 254, 141–152.
Ali, Hazrat, Khan, E., Ilahi, I., 2019. J. Chem. 6730305.
Ali, Haydar, Mukhopadhyay, S., Jana, N.R., 2019. New J. Chem. 43, 1536–1543.
Alizadeh, T., 2014. Biosens. Bioelectron. 61, 532–540.
Alizadeh, T., 2009. Electroanalysis 21, 1490–1498.
Alizadeh, T., Zare, M., Ganjali, M.R., Norouzi, P., Tavana, B., 2010. Biosens. Bioelectron. 25, 1166–1172.
Alizadeha, T., Ganjali, M.R., Norouzi, P., Zare, M., Zeraatkar, A., 2009. Talanta 79, 1197–1203.
Ansari, S., 2017. TrAC - Trends Anal. Chem. 90, 89–106.
Ansari, S., Karimi, M., 2017a. TrAC - Trends Anal. Chem. 89, 146–162.
Ansari, S., Karimi, M., 2017b. Talanta 164, 612–625.
Archer, E., Petrie, B., Kasprzyk-Hordern, B., Wolfaardt, G.M., 2017. Chemosphere 174, 437–446.
Arismendi, D., Becerra-Herrera, M., Cerrato, I., Richter, P., 2019. Talanta 201, 480–489.
Arrigo, P., Baroni, D., 2020. Sensors in Water Pollutants Monitoring: Role of Material Advanced Functional Materials and Sensors. pp. 213–231.
Aswini, K.K., Mohan, A.M.V., Biju, V.M., 2014. Mater. Sci. Eng. C 37, 321–326.
Atar, N., Yola, M.L., 2018. J. Electrochem. Soc. 165, H255–H262.
Ayankojo, A.G., Reut, J., Ciocan, V., Öpik, A., Syritski, V., 2020. Talanta 209, 120502.
Ayukekbong, J.A., Ntemgwa, M., Atabe, A.N., 2017. TAntimicrob. Resist. Infect. Control 6, 1–8.
Beduk, T., Ait-Lahcen, A., Tashkandi, N., Salama, K.N., 2020. Sensors Actuators B Chem. 314, 128026.
Belbruno, J.J., 2019. Chem. Rev. 119, 94–119.
Beldean-Galea, M.S., Vial, J., Thiébaut, D., Coman, M.V., 2020. Environ. Sci. Pollut. Res. 9535–9546.
Beluomini, M.A., da Silva, J.L., de Sá, A.C., Buffon, E., Pereira, T.C., Stradiotto, N.R., 2019. J. Electroanal. Chem. 840, 343–366.
Benedetti, B., Majone, M., Cavaliere, C., Montone, C.M., Fatone, F., Frison, N., Laganà, A., Capriotti, A.L., 2020. Microchem. J. 155, 104732.
Bilal, M., Adeel, M., Rasheed, T., Zhao, Y., Iqbal, H.M.N., 2019. Environ. Int. 124, 336–353.
Björlenius, B., Tysklind, M., Lindberg, R.H., Haglund, P., Fick, J., Ripszám, M., 2018. PSci. Total Environ. 633, 1496–1509.
Borghi, A.A., Palma, M.S.A., 2014. Brazilian J. Pharm. Sci. 50, 25–40.
Boxall, A.B.A., 2004. EMBO Rep. 5, 1110–1116.
Boyle, A., Geniès, E.M., Lapkowski, M., 1989. Synth. Met. 28, 769–774.
Boysen, R.I., 2019. J. Sep. Sci. 42, 51–71.
Cai, Y., He, X., Cui, P.L., Liu, J., Li, Z. Bin, Jia, B.J., Zhang, T., Wang, J.P., Yuan, W.Z., 2019. Food Chem. 280,

914 103–109.
915 Carvalho, F.P., 2017. Food Energy Secur. 6, 48–60.
916 Cetó, X., Saint, C.P., Chow, C.W.K., Voelcker, N.H., Prieto-Simón, B., 2016. ESensors Actuators, B Chem. 237,
917 613–620.
918 Chakraborty, I., Sathe, S.M., Khuman, C.N., Ghangrekar, M.M., 2020. Mater. Sci. Energy Technol. 3, 104–
919 115.
920 Chapman, P.M., 2007. Environ. Int. 33, 492–501.
921 Chen, H., Zhang, Z., Cai, R., Rao, W., Long, F., 2014. Electrochim. Acta 117, 385–392.
922 https://doi.org/10.1016/j.electacta.2013.11.185
923 Chen, H.J., Zhang, Z.H., Cai, R., Chen, X., Liu, Y.N., Rao, W., Yao, S.Z., 2013. Talanta 115, 222–227.
924 Chen, L., Wang, X., Lu, W., Wu, X., Li, J., 2016. Chem. Soc. Rev. 45, 2137–2211.
925 Chen, L., Xu, S., Li, J., 2011. Chem Soc Rev 40, 2922–2942.
926 Chen, Z., Tang, C., Zeng, Y., Liu, H., Yin, Z., Li, L., 2014. Anal. Lett. 47, 996–1014.
927 Cieplak, M., Kutner, W., 2016. A Trends Biotechnol. 34, 922–941.
928 Crapnell, R.D., Hudson, A., Foster, C.W., Eersels, K., van Grinsven, B., Cleij, T.J., Banks, C.E., Peeters, M.,
929 2019. Sensors (Switzerland) 19.
930 Dadkhah, S., Ziaei, E., Mehdinia, A., Baradaran Kayyal, T., Jabbari, A., 2016. Microchim. Acta 183, 1933–
931 1941.
932 Daghrir, R., Drogui, P., 2013. Environ. Chem. Lett. 11, 209–227.
933 Daughton, C.G., 2016. Sci. Total Environ. 562, 391–426.
934 Deore, B., Chen, Z., Nagaoka, T., 1999. nal. Sci. 15, 827–828.
935 Des Azevedo, S., Lakshmi, D., Chianella, I., Whitcombe, M.J., Karim, K., Ivanova-Mitseva, P.K.,
936 Subrahmanyam, S., Piletsky, S.A., 2013. Ind. Eng. Chem. Res. 52, 13917–13923.
937 Di Masi, S., Pennetta, A., Guerreiro, A., Canfarotta, F., De Benedetto, G.E., Malitesta, C., 2020. Sensors
938 Actuators, B Chem. 307, 127648.
939 Ding, S., Lyu, Z., Niu, X., Zhou, Y., Liu, D., Falahati, M., Du, D., Lin, Y., 2020. Biosens. Bioelectron. 149,
940 111830.
941 Ding, Y., Zhang, X., Yin, H., Meng, Q., Zhao, Y., Liu, L., Wu, Z., Xu, H., 2017. Sensors 17.
942 Do, M.H., Florea, A., Farre, C., Bonhomme, A., Bessueille, F., Vocanson, F., Tran-Thi, N.T., Jaffrezic-Renault,
943 N., 2015. Int. J. Environ. Anal. Chem. 95, 1489–1501.
944 Dong, S., Sun, Z., Lu, Z., 1988. Analyst 113, 1525–1528.
945 Dulio, V., Bavel, B. van, Brorström-Lundén, E., Harmsen, J., Hollender, J., Schlabach, M., Slobodnik, J.,
946 Thomas, K., Koschorreck, J., 2018. Environ. Sci. Eur. 30.
947 Ertürk, G., Mattiasson, B., 2017. Sensors (Switzerland) 17, 1–17.
948 Evgenidou, E.N., Konstantinou, I.K., Lambropoulou, D.A., 2015. Sci. Total Environ. 505, 905–926.
949 Farooq, S., Nie, J., Cheng, Y., Yan, Z., Li, J., Bacha, S.A.S., Mushtaq, A., Zhang, H., 2018. Analyst 143, 3971–
950 3989.
951 Feier, B., Blidar, A., Pusta, A., Carciuc, P., Cristea, C., 2019. Biosensors 9, 31.
952 Fekadu, S., Alemayehu, E., Dewil, R., Van der Bruggen, B., 2019. Sci. Total Environ. 654, 324–337.
953 Figueiredo, L., Erny, G.L., Santos, L., Alves, A., 2016. Talanta 146, 754–765.
954 Florea, A., Cristea, C., Vocanson, F., Səndulescu, R., Jaffrezic-Renault, N., 2015. Electrochem. commun. 59,
955 36–39.
956 Futra, D., Heng, L.Y., Jaapar, M.Z., Ulianas, A., Saeedfar, K., Ling, T.L., 2016. AAnal. Methods 8, 1381–1389.
957 García-Espinoza, J.D., Mijaylova Nacheva, P., 2019. Environ. Sci. Pollut. Res.
958 Geissen, V., Mol, H., Klumpp, E., Umlauf, G., Nadal, M., van der Ploeg, M., van de Zee, S.E.A.T.M., Ritsema,
959 C.J., 2015. Int. Soil Water Conserv. Res. 3, 57–65.
960 Ghorbani, A., Ganjali, M.R., Ojani, R., Raoof, J., 2020. Int. J. Electrochem. Sci. 15, 2913–2922.
961 Grenni, P., Ancona, V., Barra Caracciolo, A., 2018. Microchem. J. 136, 25–39.
962 Gui, R., Guo, H., Jin, H., 2019. Nanoscale Adv. 1, 3325–3363.
963 Gui, R., Jin, H., Guo, H., Wang, Z., 2018. Biosens. Bioelectron. 100, 56–70.
964 Han, Q., Shen, X., Zhu, W., Zhu, C., Zhou, X., Jiang, H., 2016. Biosens. Bioelectron. 79, 180–186.
965 Han, S., Su, L., Zhai, M., Ma, L., Liu, S., Teng, Y., 2019. J. Mater. Sci. 54, 3331–3341.
966 Holdgate, M.W., 1979. A perspective of environmental pollution. Cambridge University Press.

967 Hong, Y.J., Hong, Y.J., Liao, W., Liao, W., Yan, Z.F., Bai, Y.C., Feng, C.L., Xu, Z.X., Xu, D.Y., 2020. PJ. Chem.
968 2020, 1–12.
969 https://www.norman-network.net/?q=node/19 (Last accessed November 2019).
970 Huang, S., Xu, J., Zheng, J., Zhu, F., Xie, L., Ouyang, G., 2018. Synthesis and application of magnetic
971 molecularly imprinted polymers in sample preparation *Anal. Bioanal. Chem 3*991–4014.
972 Hutchins, R.S., Bachas, L.G., 1995. Anal. Chem. 67, 1654–1660.
973 Javid, A., Mesdaghinia, A., Nasseri, S., Mahvi, A.H., Alimohammadi, M., Gharibi, H., 2016. J. Environ. Heal.
974 Sci. Eng. 14, 1–5.
975 Kamba, P.F., Kaggwa, B., Munanura, E.I., Okurut, T., Kitutu, F.E., 2017. Pan Afr. Med. J. 27, 2–5.
976 Khadem, M., Faridbod, F., Norouzi, P., Foroushani, A.R., Ganjali, M.R., Shahtaheri, S.J., 2016. J. Iran. Chem.
977 Soc. 13, 2077–2084.
978 Khadem, M., Faridbod, F., Norouzi, P., Rahimi Foroushani, A., Ganjali, M.R., Shahtaheri, S.J., Yarahmadi, R.,
979 2017. Electroanalysis 29, 708–715.
980 Khan, S., Wong, A., Zanoni, M.V.B., Sotomayor, M.D.P.T., 2019. Mater. Sci. Eng. C 103, 109825.
981 Khanmohammadi, A., Jalili Ghazizadeh, A., Hashemi, P., Afkhami, A., Arduini, F., Bagheri, H., 2020. J. Iran.
982 Chem. Soc. 17, 2429–2447.
983 Kroon, F.J., Berry, K.L.E., Brinkman, D.L., Kookana, R., Leusch, F.D.L., Melvin, S.D., Neale, P.A., Negri, A.P.,
984 Puotinen, M., Tsang, J.J., van de Merwe, J.P., Williams, M., 2020. SSci. Total Environ. 719, 135140.
985 Kuhn, J., Aylaz, G., Sari, E., Marco, M., Yiu, H.H.P., Duman, M., 2020. S J. Hazard. Mater. 387, 121709.
986 Kumar, V., Parihar, R.D., Sharma, A., Bakshi, P., Singh Sidhu, G.P., Bali, A.S., Karaouzas, I., Bhardwaj, R.,
987 Thukral, A.K., Gyasi-Agyei, Y., Rodrigo-Comino, J., 2019. Chemosphere 236, 124364.
988 Lahcen, A.A., Amine, A., 2019. Electroanalysis 31, 188–201.
989 Lahcen, A.A., Baleg, A.A., Baker, P., Iwuoha, E., Amine, A., 2017. Sensors Actuators, B Chem. 241, 698–705.
990 Lapworth, D.J., Baran, N., Stuart, M.E., Ward, R.S., 2012. Environ. Pollut. 163, 287–303.
991 Li, C., Zeng, C., Chen, Z., Jiang, Y., Yao, H., Yang, Y., Wong, W.T., 2020. J. Hazard. Mater. 384, 121498.
992 Li, H., Wang, Y., Zha, H., Dai, P., Xie, C., 2019. Arab. J. Sci. Eng. 44, 145–152.
993 Li, J., Huang, X., Ma, J., Wei, S., Zhang, H., 2020. Ionics 26, 4183–4192
994 Li, J., Ma, F., Wei, X., Fu, C., Pan, H., 2015. Anal. Chim. Acta 871, 51–56.
995 Li, R., Feng, Y., Pan, G., Liu, L., 2019. Sensors 19.
996 Li, S., Ge, Y., Piletsky, S.A., Lunec, J., 2012. Molecularly imprinted sensors: overview and applications, 1st
997 editio. ed. Elsevier.
998 Li, S., Li, J., Ma, X., Pang, C., Yin, G., Luo, J., 2019. Biosens. Bioelectron. 139, 111321.
999 Li, Y., Xu, W., Zhao, X., Huang, Y., Kang, J., Qi, Q., Zhong, C., 2018. Analyst 143, 5094–5102.
1000 Li, Y., Zhang, L., Dang, Y., Chen, Z., Zhang, R., Li, Yingchun, Ye, B.C., 2019. Biosens. Bioelectron. 127, 207–
1001 214. h
1002 Liang, M., Xian, Y., Wang, B., Hou, X., Wang, L., Guo, X., Wu, Y., Dong, H., 2020. Environ. Pollut. 263,
1003 114389.
1004 Liang, Y., Yu, L., Yang, R., Li, X., Qu, L., Li, J., 2017. Sensors Actuators, B Chem. 240, 1330–1335.
1005 Liu, G., Huang, X., Li, L., Xu, X., Zhang, Y., Lv, J., Xu, D., 2019. Nanomaterials 9, 1–19.
1006 Liu, L., Zhu, X., Zeng, Y., Wang, H., Lu, Y., Zhang, J., Yin, Z., Chen, Z., Yang, Y., Li, L., 2018. Polymers. 10, 1–13.
1007 Liu, Y., Zhu, L., Luo, Z., Tang, H., 2013. Sensors Actuators, B Chem. 185, 438–444.
1008 Lopes, F., Pacheco, J.G., Rebelo, P., Delerue-Matos, C., 2017. Sensors Actuators, B Chem. 243, 745–752.
1009 Luliński, P., 2017. Mater. Sci. Eng. C 76, 1344–1353.
1010 Luo, Y., Guo, W., Ngo, H.H., Nghiem, L.D., Hai, F.I., Zhang, J., Liang, S., Wang, X.C., 2014. Sci. Total Environ.
1011 473–474, 619–641.
1012 Luong, J.H.T., Male, K.B., Glennon, J.D., 2009. Analyst 134, 1965–1979.
1013 Madikizela, L., Tavengwa, N., Pakade, V., 2018. Recent Res. Polym.
1014 Madikizela, L.M., Tavengwa, N.T., Chimuka, L., 2018. J. Pharm. Biomed. Anal. 147, 624–633.
1015 Maduraiveeran, G., Sasidharan, M., Ganesan, V., 2018. Biosens. Bioelectron. 103, 113–129.
1016 Malitesta, C., Losito, I., Zambonin, P.G., 1999. Anal. Chem. 71, 1366–1370.
1017 Manisalidis, I., Stavropoulou, E., Stavropoulos, A., Bezirtzoglou, E., 2020. Front. Public Heal. 8, 1–13.
1018 Maria G.C., A., K B, A., Rison, S., Varghese, A., George, L., 2020. Synth. Met. 261, 116309.
1019 Mayes, A.G., Whitcombe, M.J., 2005. Adv. Drug Deliv. Rev. 57, 1742–1778.

1020 Mercurio, P., Flores, F., Mueller, J.F., Carter, S., Negri, A.P., 2014. Mar. Pollut. Bull. 85, 385–390.
1021 Merlo, F., Speltini, A., Maraschi, F., Sturini, M., Profumo, A., 2020. Arab. J. Chem. 13, 4673–4680. h
1022 Miege, C., Choubert, J.M., Ribeiro, L., Eusèbe, M., Coquery, M., 2009. Environ. Pollut. 157, 1721–1726.
1023 Moein, M.M., Abdel-Rehim, A., Abdel-Rehim, M., 2019. Recent Applications of Molecularly Imprinted.
1024 Molecules 24, 1–12.
1025 Mokhtari, P., Ghaedi, M., 2019. Eur. Polym. J. 118, 614–618.
1026 Motaharian, A., Motaharian, F., Abnous, K., Hosseini, M.R.M., Hassanzadeh-Khayyat, M., 2016. Anal.
1027 Bioanal. Chem. 408, 6769–6779.
1028 Motia, S., Albert, I., Popescu, L.M., Mioara, R., Bouchikhi, B., El, N., 2018. J. Electroanal. Chem. 823, 553–
1029 562.
1030 Motia, S., Tudor, I.A., Ribeiro, P.A., Raposo, M., Bouchikhi, B., El Bari, N., 2019. Sci. Total Environ. 664, 647–
1031 658.
1032 Mujahid, A., Lieberzeit, P.A., Dickert, F.L., 2010. Materials. 3, 2196–2217.
1033 Mzukisi, L., Tawanda, N., Tutu, H., Chimuka, L., Madikizela, L.M., Tavengwa, N.T., Tutu, H., Chimuka, L.,
1034 2018. Anal. Chem. 17, 14–22. h
1035 Naidu, R., Arias Espana, V.A., Liu, Y., Jit, J., 2016. Chemosphere 154, 350–357.
1036 Namieśnik, J., 2000. Crit. Rev. Anal. Chem. 30, 221–269.
1037 Nsibande, S.A., Forbes, P.B.C., 2019. Luminiscence 480–488.
1038 Özcan, A., Topçuoğulları, D., 2017. Sensors Actuators, B Chem. 250, 85–90.
1039 Pacheco, J.G., Rebelo, P., Freitas, M., Nouws, H.P.A., Delerue-Matos, C., 2018. Sensors Actuators, B Chem.
1040 273, 1008–1014.
1041 Paíga, P., Correia, M., Fernandes, M.J., Silva, A., Carvalho, M., Vieira, J., Jorge, S., Silva, J.G., Freire, C.,
1042 Delerue-Matos, C., 2019. Sci. Total Environ. 648, 582–600.
1043 Paíga, P., Santos, L.H.M.L.M., Ramos, S., Jorge, S., Silva, J.G., Delerue-Matos, C., 2016. Sci. Total Environ.
1044 573, 164–177.
1045 Patel, M., Kumar, R., Kishor, K., Mlsna, T., Pittman, C.U., Mohan, D., 2019. Chem. Rev. 119, 3510–3673.
1046 Petrie, B., Barden, R., Kasprzyk-Hordern, B., 2014. Water Res. 72, 3–27.
1047 Pohanka, M., 2017. Int. J. Electrochem. Sci. 12, 8082–8094.
1048 Prasad, B.B., Fatma, S., 2016. Sensors Actuators, B Chem. 229, 655–663.
1049 Prasad, B.B., Jauhari, D., Tiwari, M.P., 2014. Biosens. Bioelectron. 59, 81–88.
1050 Prasad, B.B., Singh, K., 2016. Electrochim. Acta 187, 193–203.
1051 Rahim, S., Bhayo, A.M., Shah, M.R., Malik, M.I., 2019. Microchem. J. 149, 104048.
1052 Ramírez-Malule, H., Quiñones-Murillo, D.H., Manotas-Duque, D., 2020. Emerg. Contam. 6, 179–193.
1053 Rao, H., Liu, X., Ding, F., Wan, Y., Zhao, X., Liang, R., Zou, P., Wang, Y., Wang, X., Zhao, Q., 2018. Chem. Eng.
1054 J. 338, 478–487.
1055 Rasheed, T., Bilal, M., Nabeel, F., Adeel, M., Iqbal, H.M.N., 2019. Environ. Int. 122, 52–66.
1056 Rebelo, P., Pacheco, J.G., Cordeiro, M.N.D.S., Melo, A., Delerue-Matos, C., 2020. Anal. Methods 12.
1057 Ribeiro, A.R., Sures, B., Schmidt, T.C., 2018. Environ. Pollut. 241, 1153–1166.
1058 Richardson, S.D., Ternes, T.A., 2014. Anal. Chem. 86, 2813–2848.
1059 Rivera-Jaimes, J.A., López de Alda, M., Aceña, J., Melgoza-Alemán, R.M., Postigo, C., Barceló, D., 2018. Sci.
1060 Total Environ. 613–614, 1263–1274.
1061 Rousis, N.I., Bade, R., Bijlsma, L., Zuccato, E., Sancho, J. V., Hernandez, F., Castiglioni, S., 2017. Environ. Res.
1062 156, 31–38.
1063 Sadki, S., Schottland, P., Brodie, N., Sabouraud, G., 2000. Chem. Soc. Rev. 29, 283–293.
1064 Sadriu, I., Bouden, S., Nicolle, J., Podvorica, F.I., Bertagna, V., Berho, C., Amalric, L., Vautrin-Ul, C., 2020.
1065 Talanta 207, 120222.
1066 Salste, L., Leskinen, P., Virta, M., Kronberg, L., 2007. Sci. Total Environ. 378, 343–351.
1067 Sarafraz-Yazdi, A., Amiri, A., Rounaghi, G., Eshtiagh-Hosseini, H., 2012. Anal. Chim. Acta 720, 134–141.
1068 Sarpong, K.A., Zhang, K., Luan, Y., Cao, Y., Xu, W., 2020. Microchem. J. 154, 104526.
1069 Sayyahmanesh, M., Asgari, S., Meibodi, A.S.E., Ahooyi, T.M., 2016. arXiv:1604.07853.
1070 Shaheen, A., Munawar, A., Tahir, M.A., Khan, W.S., Lieberzeit, P.A., Bajwa, S.Z., 2017. J. Hazard. Mater. 342,
1071 96–106.
1072 Sharma, G., Kandasubramanian, B., 2020. J. Chem. Eng. Data 65, 396–418.

Sharma, P.S., Pietrzyk-Le, A., D'Souza, F., Kutner, W., 2012. Anal. Bioanal. Chem. 402, 3177–3204.
Shi, T., Tan, L., Fu, H., Wang, J., 2019. Mar. Pollut. Bull. 146, 591–597.
Shirzadmehr, A., Rezaei, M., Bagheri, H., Khoshsafar, H., 2016. Anal. Chem. 96, 929–944.
Silva, V., Montanarella, L., Jones, A., Fernández-Ugalde, O., Mol, H.G.J., Ritsema, C.J., Geissen, V., 2018. Sci. Total Environ. 621, 1352–1359.
Sobiech, M., Bujak, P., Lulinski, P., Pron, A., 2019. Nanoscale 11, 12030–12074.
Spietelun, A., Marcinkowski, Ł., de la Guardia, M., Namieśnik, J., 2013. J. Chromatogr. A 1321, 1–13.
Sui, Q., Cao, X., Lu, S., Zhao, W., Qiu, Z., Yu, G., 2015. Emerg. Contam. 1, 14–24.
Surya, S.G., Khatoon, S., Ait Lahcen, A., Nguyen, A.T.H., Dzantiev, B.B., Tarannum, N., Salama, K.N., 2020. RSC Adv. 10, 12823–12832.
Tadi, K.K., Motghare, R. V., Ganesh, V., 2014. Electroanalysis 26, 2328–2336.
Tan, F., Cong, L., Li, X., Zhao, Q., Zhao, H., Quan, X., Chen, J., 2016. Sensors Actuators, B Chem. 233, 599–606.
Tao, Q., Li, B., Li, Q., Han, X., Jiang, Y., Jupa, R., Wang, C., Li, T., 2019. Sci. Total Environ. 659, 1448–1456.
Toro, M.J.U., Marestoni, L.D., Del Pilar Taboada Sotomayor, M., 2015. Sensors Actuators, B Chem. 208, 299–306. h
Uzun, L., Turner, A.P.F., 2016. Biosens. Bioelectron. 76, 131–144.
Van, T.T.H., Yidana, Z., Smooker, P.M., Coloe, P.J., 2020. AJ. Glob. Antimicrob. Resist. 20, 170–177.
Vinokurov, I.A., 1992. Sensors Actuators B. Chem. 10, 31–35.
Vytřas, K., Švancara, I., Metelka, R., 2009. J. Serbian Chem. Soc. 74, 1021–1033.
Wackerlig, J., Schirhagl, R., 2016. Anal. Chem. 88, 250 - 261
Wang, X., Ding, H., Yu, X., Shi, X., Sun, A., Li, D., Zhao, J., 2019. Talanta 197, 98–104.
Wang, Y., Yang, Y., Xu, L., Zhang, J., 2011. Bisphenol Electrochim. Acta 56, 2105–2109.
Wong, A., Foguel, M.V., Khan, S., Oliveira, F.M. De, Tarley, C.R.T., Sotomayor, M.D.P.T., 2015. Electrochim. Acta 182, 122–130.
Wu, B., Hou, L., Du, M., Zhang, T., Xue, Z., Lu, X., 2014. RSC Adv. 4, 53701–53710.
Wulff, G., Sarhan, A., 1972. TAngew. Chem. Int. Ed. Engl. 11, 341–343.
Xiao, D., Jiang, Y., Bi, Y., 2018. Microchim Acta 185
Xiao, L., Zhang, Z., Wu, C., Han, L., Zhang, H., 2017. Food Chem. 221, 82–86.
Xie, C., Gao, S., Guo, Q., Xu, K., 2010a. Microchim. Acta 169, 145–152.
Xie, C., Li, H., Li, S., Wu, J., Zhang, Z., 2010b. Anal. Chem. 82, 241–249.
Xie, L., Xiao, N., Li, L., Xie, X., Li, Y., 2020. Int. J. Mol. Sci. 21, 4139.
Xu, J., Zhang, R., Liu, C., Sun, A., Chen, J., Zhang, Z., Shi, X., 2020. Sensors 20, 884.
Xu, L., Li, J., Zhang, J., Sun, J., Gan, T., Liu, Y., 2020. Analyst.
Xu, W., Wang, Q., Huang, W., Yang, W., 2017. J. Sep. Sci. 40, 4839–4846.
Xue, X., Wei, Q., Wu, D., Li, H., Zhang, Y., Feng, R., Du, B., 2014. Electrochim. Acta 116, 366–371.
Yang, S., Wang, Y., Jiang, Y., Li, S., Liu, W., 2016. Polymers (Basel). 8.
Yang, Y., Fang, G., Liu, G., Pan, M., Wang, X., Kong, L., He, X., Wang, S., 2013. EBiosens. Bioelectron. 47, 475–481.
Yang, Y., Ok, Y.S., Kim, K.H., Kwon, E.E., Tsang, Y.F., 2017. Sci. Total Environ. 596–597, 303–320.
Yaroshenko, I., Kirsanov, D., Marjanovic, M., Lieberzeit, P.A., Korostynska, O., Mason, A., Frau, I., Legin, A., 2020. Sensors 20, 1–23.
Ye, L., 2013. Molecular Imprinting: Principles and Applications of Micro- and Nanostructure Polymers. CRC Press: Boca Raton, FL, USA.
Yola, M.L., Atar, N., 2017. J. Electrochem. Soc. 164, B223–B229.
Yu, R., Zhou, H., Li, M., Song, Q., 2019. J. Electroanal. Chem. 832, 129–136.
Yuan, L., Zhang, J., Zhou, P., Chen, J., Wang, R., Wen, T., Li, Y., Zhou, X., Jiang, H., 2011. Biosens. Bioelectron. 29, 29–33.
Zaidi, S.A., 2017. Biomater. Sci. 5, 388–402.
Zamora-Gálvez, A., Ait-Lahcen, A., Mercante, L.A., Morales-Narváez, E., Amine, A., Merkoçi, A., 2016. Anal. Chem. 88, 3578–3584.
Zamora-Gálvez, A., Mayorga-Matinez, C.C., Parolo, C., Pons, J., Merkoçi, A., 2017. Electrochem. commun. 82, 6–11.

Zhang, B., Fan, X., Zhao, D., 2019. Polymers (Basel). 11, 1–21.
Zhang, C., She, Y., Li, T., Zhao, F., Jin, M., Guo, Y., Zheng, L., Wang, S., Jin, F., Shao, H., Liu, H., Wang, J., 2017. Anal. Bioanal. Chem. 409, 7133–7144.
Zhang, J., Lei, J., Ju, H., Wang, C., 2013. Anal. Chim. Acta 786, 16–21.
Zhang, R., Zhang, G., Zheng, Q., Tang, J., Chen, Y., Xu, W., Zou, Y., Chen, X., 2012. Ecotoxicol. Environ. Saf. 80, 208–215.
Zhang, R.R., Zhan, J., Xu, J.J., Chai, J.Y., Zhang, Z.M., Sun, A.L., Chen, J., Shi, X.Z., 2020. Sensors Actuators, B Chem. 317, 128237.
Zhao, H., Chen, Y., Tian, J., Yu, H., Quan, X., 2012. J. Electrochem. Soc. 159, J231–J236.
Zhao, Y., Yuan, F., Quan, X., Yu, H., Chen, S., Zhao, H., Liu, Z., Hilal, N., 2015. Anal. Methods 7, 2693–2698.
Zhou, T., Ding, L., Che, G., Jiang, W., Sang, L., 2019. Trends Anal. Chem. 114, 11–28.
Zhou, T., Feng, Y., Zhou, L., Tao, Y., Luo, D., Jing, T., Shen, X., Zhou, Y., Mei, S., 2016. Sensors Actuators, B Chem. 236, 153–162.
Zhou, T., Halder, A., 2018. Biosensors
Zhu, L., Cao, Y., Cao, G., 2014. Biosens. Bioelectron. 54, 258–261.
Zulkifli, S.N., Rahim, H.A., Lau, W.J., 2018. Sensors Actuators, B Chem. 255, 2657–2689.